New Mexico Geological Society

Downloaded from: https://nmgs.nmt.edu/publications/guidebooks/55



The San Luis Basin to the Española Basin - Third-day Road Log from Talpa to the Rio Grande del Rancho Valley, U.S. Hill, Vadito, and Peñasco

Paul W. Bauer, Adam S. Read, Keith I. Kelson, Barry S. Kues, Scott B. Aby, Wiliam R. Muehlberger, Ren A. Thompson, George S. Austin, and Gary A. Smith

2004, pp. 77-98. https://doi.org/10.56577/FFC-55.77

in:

Geology of the Taos Region, Brister, Brian; Bauer, Paul W.; Read, Adam S.; Lueth, Virgil W.; [eds.], New Mexico Geological Society 55 th Annual Fall Field Conference Guidebook, 440 p. https://doi.org/10.56577/FFC-55

This is one of many related papers that were included in the 2004 NMGS Fall Field Conference Guidebook.

Annual NMGS Fall Field Conference Guidebooks

Every fall since 1950, the New Mexico Geological Society (NMGS) has held an annual Fall Field Conference that explores some region of New Mexico (or surrounding states). Always well attended, these conferences provide a guidebook to participants. Besides detailed road logs, the guidebooks contain many well written, edited, and peer-reviewed geoscience papers. These books have set the national standard for geologic guidebooks and are an essential geologic reference for anyone working in or around New Mexico.

Free Downloads

NMGS has decided to make peer-reviewed papers from our Fall Field Conference guidebooks available for free download. This is in keeping with our mission of promoting interest, research, and cooperation regarding geology in New Mexico. However, guidebook sales represent a significant proportion of our operating budget. Therefore, only *research papers* are available for download. *Road logs*, *mini-papers*, and other selected content are available only in print for recent guidebooks.

Copyright Information

Publications of the New Mexico Geological Society, printed and electronic, are protected by the copyright laws of the United States. No material from the NMGS website, or printed and electronic publications, may be reprinted or redistributed without NMGS permission. Contact us for permission to reprint portions of any of our publications.

One printed copy of any materials from the NMGS website or our print and electronic publications may be made for individual use without our permission. Teachers and students may make unlimited copies for educational use. Any other use of these materials requires explicit permission.

This page is intentionally left blank to maintain order of facing pages.

THE SAN LUIS BASIN TO THE ESPAÑOLA BASIN
THIRD-DAY ROAD LOG FROM TALPA TO THE RIO GRANDE DEL RANCHO VALLEY, U.S. HILL, VADITO, AND PEÑASCO

PAUL W. BAUER, ADAM S. READ, KEITH I. KELSON, BARRY S. KUES, SCOTT B. ABY, WILLIAM R. MUEHLBERGER, REN A. THOMPSON, GEORGE S. AUSTIN, AND GARY A. SMITH

Assembly Point: Sagebrush Inn, Taos

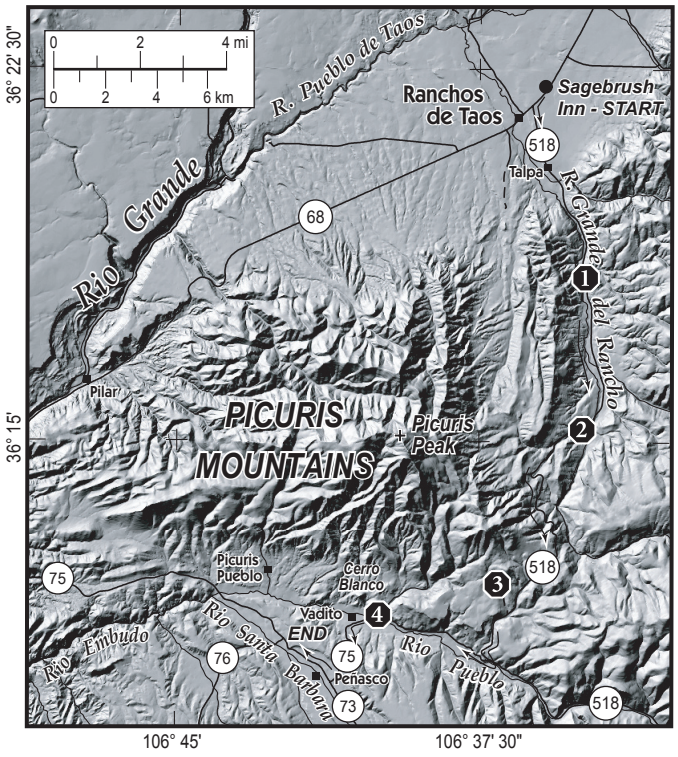
Departure Time: 7:30 AM

Distance: 23.6 miles

Three stops plus one optional stop

SUMMARY

The last day of the conference begins in Taos and ends in Peñasco. On this tour we continue to explore the important Cenozoic structures and deposits in the southeastern San Luis Basin, including the pre- to early-rift Picuris Formation, the repeatedly reactivated Picuris-Pecos fault system, and late Laramide grabens. We will also stop to examine the superbly exposed fossiliferous Pennsylvanian strata near Talpa and discuss Ancestral Rockies sedimentation in the Taos trough. An optional stop at the mica mine near Vadito provides a look at the Proterozoic Rio Pueblo schist and a unique and controversial mining operation. The trip will end on Picuris Pueblo Tribal lands on a spectacular exposure of the Picuris Formation where we discuss early Cenozoic sedimentation and paleogeography as well as development of the Peñasco embayment. A supplemental log continues this tour from Peñasco south along the scenic high road to Española and points south.



0.0 Depart from the southwest entrance of the [1] Sagebrush Inn.

Turn right onto NM-68 towards Ranchos de Taos. **0.0**

0.5 **Turn left onto NM-518 towards Talpa**. Between this **[43]** intersection and the village of Talpa, the highway is on Pleistocene alluvial-fan deposits derived from the Rio Grande del Rancho drainage and adjacent range-front tributaries. To the right, the broad Rio Grande del Rancho valley is flanked by the late Pleistocene Qt4 terrace (on this eastern side of the river) and the middle Pleistocene Qt2 terrace (on the western side of the river). The suspiciously straight Rio Grande del Rancho valley (Fig. 3.1) is parallel to mapped Laramide faults of the Picuris-Pecos fault system and is probably developed on a major buried fault that has bedrock exposures at the north and south ends of the valley (Bauer et al., 1999b). **0.5**

1.2 Colorful cemetery (Campo Santo) on left. **0.7**

1.7 Enter village of Talpa ("knob" in Spanish). Europeans probably settled in this area in the 1780s. The village contains a remarkable variety of traditionally constructed historic adobe homes and churches. Set back off the highway on the right are the remains of a private chapel named Our Lady of Talpa, which was built as a private oratory in 1838 by Don Nicolas Sandoval. Other historic buildings on the right include a 19th-century hacienda and a Campo Santo (Spanish, "cemetery"). The Talpa plaza contains Our Lady of San Juan de los Lagos church, a beautiful little adobe church built in 1828. Talpa also contains a *morada* (Spanish, "meeting place") which was used as a meeting hall by the Penitente Brotherhood, and a plastered adobe *torreon* (Spanish, "large defense tower") which was used as a defensive refuge by Spanish settlers. This is one of the few remaining *torreons* in New Mexico. **0.5**



FIGURE 3.1. View northward down the Rio Grande del Rancho valley. The linearity of this valley is controlled by a north-striking set of high-angle faults of the Rio Grande del Rancho fault zone, which consists of several sub-parallel faults that offset rocks as young as the Miocene Picuris Formation.

2.0 Talpa Elementary School on left near Milepost 71. For the next 10 miles, NM-518 travels south along the meandering Rio Grande del Rancho, flows through a relatively broad, flat-floored valley developed in Pennsylvanian sedimentary rocks. The Rio Grande del Rancho is associated with relatively low amounts of surface water discharge for its large drainage area, which is attributable to relatively permeable bedrock and substantial storage of snowmelt and thunderstorm runoff (Kelson, 1986). **0.3**

2.6 Leaving Talpa. Forest Road 437 on left leads to the valley of the Rio Chiquito, along which are thick, fossiliferous exposures of the Flechado Formation. North-down strands of the Embudo fault exist under the road here, and continue northeastward through the bench on the skyline at 9:00 and westward along the Picuris Mountains piedmont. At 2:30, the bare slopes across the Rio Grande del Rancho are exposures of the lower conglomerate member of the Picuris Formation, which consists of green, red, and yellow clay-rich siltstone that contains a 10-cm-thick, coarse-grained, white tephra. The $^{40}Ar/^{39}Ar$ date of 34.64 ± 0.16 Ma (Aby et al., 2004, this volume), based on analysis of 15 sanidine crystals, most likely represents the eruptive age of a near-source ash. The source of the ash is unknown, although possibilities include the Rock House Canyon Tuff (34.4 Ma), the Kneeling Nun Tuff (34.9 Ma), the Datil Well Tuff (35.0 Ma), and the tuff of Steins (34.4 Ma) (W. McIntosh, personal commun., 2004). **0.6**

2.7 Entering valley of the Rio Grande del Rancho as we cross the principal mountain front exposure of the Embudo fault (Fig 3.2). This drainage represents the gradual transitional zone between the Embudo fault and the Sangre de Cristo fault. Slickenlines on faults in this area show oblique (left-lateral, north-down) slip. Roadcuts on left are predominantly dark gray marine shales of the upper part of the Flechado Formation. Ahead, Pennsylvanian rocks are on both sides of the road, although the high ridge on right is composed of quartzite-cobble conglomerate that Bauer and Kelson (2004a, this volume) interpreted as lowermost Picuris Formation (equivalent to the Bradley conglomerate near Pilar that was discussed in the Day 2 road log). Aby et al. (2004, this volume) have renamed the lower part of the Picuris Formation the lower conglomerate member. **0.1**

3.8 "Entering Carson National Forest" sign. Flechado Formation exposures on the left for next 0.8 miles are the source of one of the most diverse, well-preserved, Middle Pennsylvanian faunas in North America (see Minipaper by Kues and Fig. 3.3). **1.1**

3.9 Steep dip of the Pennsylvanian strata in the roadcut to the left is due to our proximity of a major strand of the Picuris-Pecos fault system, named the Rio Grande del Rancho fault by Bauer et al. (1999). **0.1**

4.6 Road bends to left. The paved pullout to the right is an alternate parking area for an examination of the roadcut at STOP 1. McGaffey Ridge, the high ridge to the west, is composed of steeply east-dipping Mississippian rocks of the Arroyo Peñasco Group, the oldest Paleozoic sedimentary rocks in north-central New Mexico. These carbonate rocks have experienced a complex diagenetic history of alteration that is due to at least four sea-level fluctuations resulting in repeated subaerial exposure (Ulmer and Laury, 1984). **0.7**

4.7 North end of a long roadcut that exposes the Flechado Formation. **0.1**

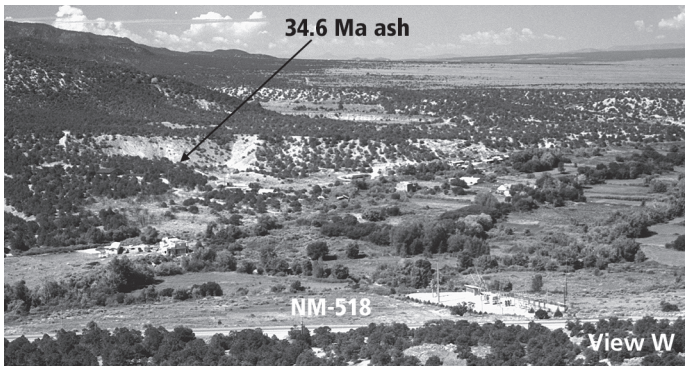


FIGURE 3.2. Vista west across the Rio Grande del Rancho and NM-518 from the Pennsylvanian ridge south of Talpa. The slope break at the top of the Picuris Mountains piedmont is the trace of one of the numerous fault strands of the Embudo fault zone. The light-colored slopes in the middle distance are siltstones and sandstones of the lower conglomeratic member of the Picuris Formation. An ash interbedded with those sedimentary rocks was dated at 34.6 Ma, and established the late Eocene age of the oldest known Picuris Formation.

PALEONTOLOGY OF THE UPPER FLECHADO FORMATION NEAR TALPA, NORTH-CENTRAL NEW MEXICO

Barry S. Kues
Department of Earth and Planetary Sciences, University of New Mexico, Albuquerque, NM 87131

The thick, dark-gray shale sequence of the upper (Desmoinesian) part of the Flechado Formation south of Talpa contains one of the most diverse and best-preserved Pennsylvanian marine faunas in North America. This fauna differs from most Pennsylvanian faunas in New Mexico in being derived from prodeltaic to interdistributary bay environments rather than from carbonate shelf limestones and calcareous shales, and in being dominated by molluscs, particularly gastropods and bivalves, rather than by more stenotopic groups such as brachiopods, bryozoans, corals, fusulinids, and echinoderms, although all of these groups are present and may be locally abundant. The fauna is also unusual in being represented by vast numbers of individual specimens and by being easy to collect, as the specimens erode intact from the soft shale. More than 20 years ago, when I began collecting here, one could sit in one place in the shade of a pine tree and collect a hundred or more good specimens before moving a few feet away. However, the more accessible exposures are now almost barren of fossils because of recent and apparently heavy collecting pressure.

The first geologist to sample this rich Middle Pennsylvanian invertebrate fauna, ironically, was the famed vertebrate paleontologist Edward D. Cope, a member of the Wheeler Expedition of 1874. Cope (1875, p. 66) followed the valley of "Rancho Creek" (Rio Grande del Rancho) for about 8 miles, riding close to the present route of NM-518, noted "great numbers of characteristic fossils, weathered out and beautifully preserved", and made a small collection of specimens. These were given to C. A. White, who listed about 50 taxa and described several new species (White, 1881), but no subsequent collections of this rich fauna were made for more than 60 years. The first modern study of the fauna of the Flechado Formation near Talpa was by Young (1945a), who, in an unpublished doctoral dissertation for Harvard, reported nearly 150 invertebrate taxa. Several nautiloid cephalopods and a new giant scaphopod were described in publications (Young, 1942, 1945b), but most of the fauna remained unpublished.

Sutherland and Harlow (1973) described the brachiopods of the Sangre de Cristo range, but few were from upper Flechado exposures as far north as Talpa. However, more than 30 species of brachiopods have more recently been identified from this area. They are less diverse than gastropods or bivalves, but some shale units contain large numbers of the small chonetoid *Mesolobus* and brachiopods may be conspicuous in some beds of argillaceous limestones within the predominantly shale sequence. Common Flechado brachiopod species from exposures along today's route are illustrated here (Fig. 3.3), both because they have not previously been figured and because the brachiopods are excellent indicators of the early Desmoinesian age of these Flechado exposures.

Gastropods (snails) are especially diverse and common in this fauna, to an extent found in few other North American Pennsylvanian localities. Kues (1990) described several new genera and species, and Kues and Batten (2001) described the entire gastropod fauna, incorporating thousands of microgastropods retrieved from bulk sediment samples. More than 150 species, including four new genera and 22 new species, are now known from the Flechado exposures south of Talpa. The most common gastropods are the low-spired, strongly nodose neritoid *Trachydomia*; *Taosia*, a high-spired, carinate genus; the small, conical *Euconodoma*; the small, very-low-spired *Anomphalus*; the low-spired pleurotomarioids *Glabrocingulum*, *Worthenia*, and *Trepospira*; and the microgastropods *Donaldina* and *Girtyspira*.

Bivalves are not nearly as abundant as gastropods, but are fairly diverse, with more than 40 species recognized. Small nuculoids (especially *Nuculopsis*), and two species of *Astartella*, a rather plump, oval genus with strong concentric ridges across the valves, are the most abundant bivalves. Kues (1984) illustrated some of the most common bivalves, and full description of the entire bivalve fauna is in progress. The high diversity and numbers of gastropods and bivalves indicates that the Flechado environment was optimum for these molluscs. The prodelta and interdistributary bay environments represented by the dark-gray shales received much organic material from the nearby fan-delta systems, which accumulated on and in the sediments, supporting a large biomass of grazing, sediment-feeding, and suspension-feeding organisms. Other molluscs, such as rostroconchs (under study), scaphopods, both straight-coned and planispirally coiled nautiloid cephalopods, and even chitons (Kues, 1983) are also present in these Flechado shale beds.

Other groups of invertebrates are also present, although generally not in large numbers, and most have not yet been intensively studied. These include fusulinids, sponges, conularids (small, pyramidal organisms with phosphatic shells that may be related to jellyfish), solitary rugose and colonial tabulate corals, and bryozoans, crinoids, and echinoids. Examination of bulk sediment samples yielded microscopic plates and other skeletal elements of ophiuroids (brittle stars), holothuroids (sea cucumbers), echinoids and crinoids, as well as diverse ostracods and non-fusulinid foraminifers (Kietzke, 1990). Trilobites are rare, and are described by Kues (2004, this guidebook).

Finally, veretebrate remains are also present in the Flechado. Fish remains include small teeth and dermal denticles of sharks

and paleoniscoids (Kietzke, 1990), and several genera of larger chondrichthyan (sharks and allies) teeth and dermal denticles were described by Zidek and Kietzke (1993). Surprisingly, a fragment of a femur of a terrestrial vertebrate, an early captirhinomorph reptile, was also recovered from the Flechado shales (Lucas and Hunt, 1991), having presumedly washed into the marine environment from the nearby land.

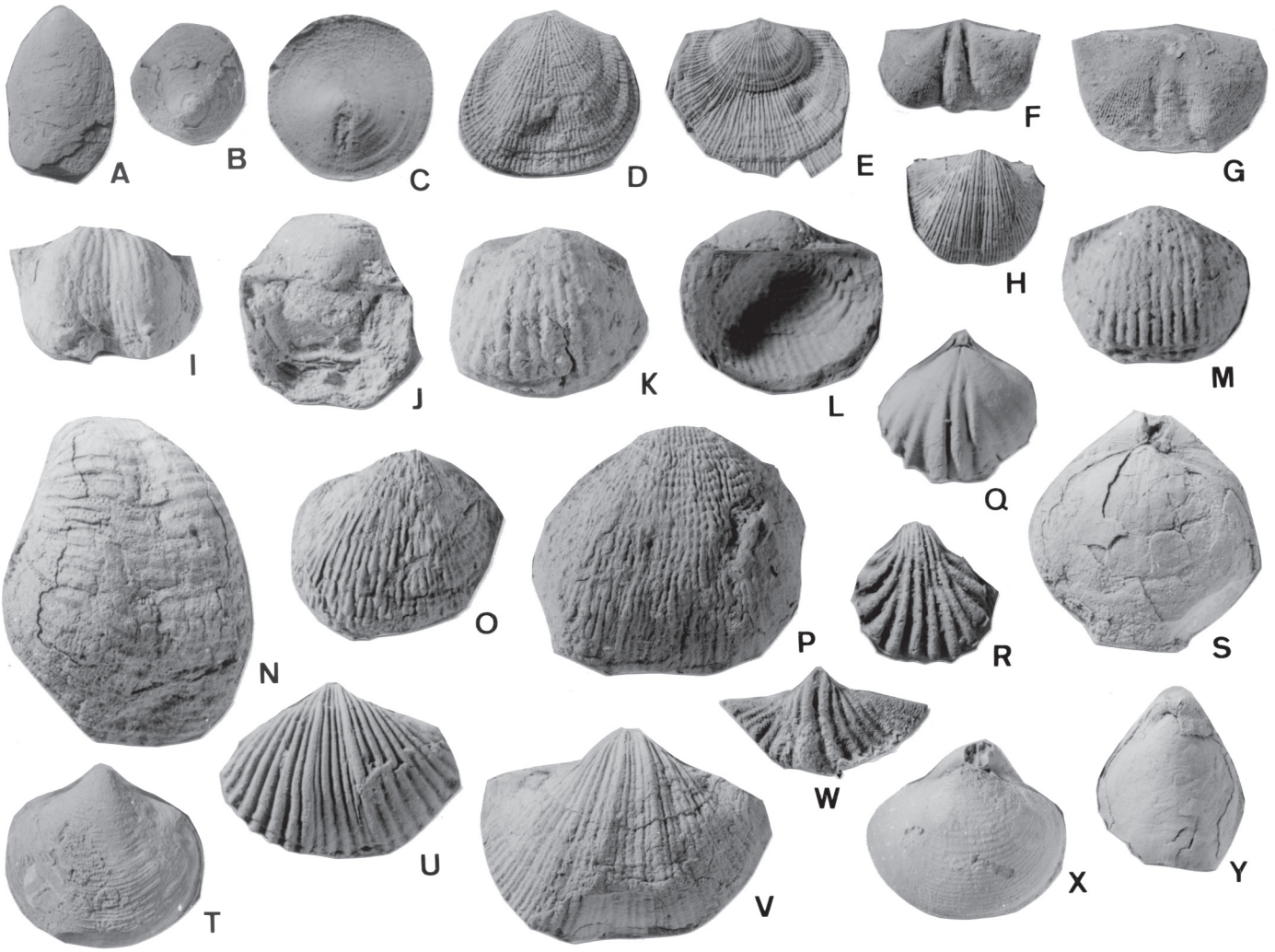


FIGURE 3.3. Characteristic Desmoinesian brachiopods from the upper part of the Flechado Formation, south of Talpa, New Mexico. **A**, *Lingula* cf. *L. carbonaria* Shumard, brachial valve, UNM 13,420, x2.25. **B, C,** *Orbiculoidea missouriensis* (Shumard), brachial valve, UNM 13,421 (x2.50) and pedicle valve, UNM 13,422 (x2). **D,** *Rhipidomella* sp., brachial valve, UNM 13,423, x2.25. **E,** *Derbyia crassa* (Meek and Hayden), incomplete pedicle valve, UNM 13,424, x1. **F,** *Mesolobus profundus* Sutherland and Harlow, small pedicle valve, UNM 13,425, x2. **G,** *Mesolobus striatus* Weller and McGehee, pedicle valve, UNM 13,426, x2. **H,** *Chonetinella jeffordsi* Stevens, pedicle valve, UNM 13,427, x2. **I, J,** *Kozlowskia haydenensis* (Girty), pedicle valve, UNM 13,428, and brachial valve view, UNM 13,429, x1.5. **K, L,** *Desmoinesia muricatina* (Girty), pedicle valve, UNM 13,430, and brachial valve view, UNM 13,431, x2. **M,** *Desmoinesia* aff. *D. missouriensis* (Girty), pedicle valve, UNM 13,432, x2. **N,** *Echinaria* cf. *E. knighti* (Dunbar and Condra), pedicle valve, UNM 13,433, x1. **O,** *Buxtonia* n. sp., incomplete pedicle valve, UNM 13,434, x1.5. **P,** *Antiquatonia hermosana* (Girty), pedicle valve, UNM 13,435, x1. **Q,** *Wellerella* aff. *W. osagensis* (Swallow), brachial valve, UNM 13,436, x2. **R,** *Hustedia mormoni* (Marcou), somewhat flattened pedicle valve, UNM 13,437, x2.25. **S,** *Composita subtilita* (Hall), brachial valve view of *C.* "*ovata*" morph, UNM 13,438, x1. **T,** *Cleiothyridina pecosii* (Marcou), pedicle valve, UNM 13,439, x2. **U,** *Anthracospirifer curvilateralis chavezae* Sutherland and Harlow, pedicle valve, UNM 13,440, x1.25. **V,** *Neospirifer cameratus* (Morton), pedicle valve, UNM 13,441, x1. **W,** *Punctospirifer kentuckyensis* (Shumard), pedicle valve, UNM 13,442, x2. **X,** *Phricodothyris perplexa* (McChesney), brachial valve view, UNM 13,443, x1.5. **Y,** *Beecheria* aff. *B. bovidens* (Morton), brachial valve view, UNM 13,444, x1.

REFERENCES

Cope, E. D., 1875, Report on the geology of that part of northwestern New Mexico examined during the field season of 1874; *in* Annual report upon the geographical explorations and surveys west of the one-hundredth meridian [Wheeler Survey]: Appendix LL of the Annual Report of the Chief of Engineers for 1875, p. 61-97.

Kietzke, K. K., 1990, Microfossils from the Flechado Formation (Pennsylvanian, Desmoinesian) near Talpa, New Mexico: New Mexico Geological Society, 41st Fall Field Conference, Guidebook, p. 259-276.

Kues, B. S., 1983, A chiton from the Flechado Formation (Middle Pennsylvanian) of Northern New Mexico: New Mexico Journal of Science, v. 23, p. 19-22.
Kues, B. S., 1984, Pennsylvanian stratigraphy and paleontology of the Taos area, north-central New Mexico: New Mexico Geological Society, 35th Field Confernce, Guidebook, p. 107-114.
Kues, B. S., 1990, New and little known Middle Pennsylvanian gastropods from the Flechado Formation, Taos County, New Mexico: New Mexico Geological Society, 41st Fall Field Conference, Guidebook, p. 251-258.
Kues, B.S., 2004, Pennsylvanian trilobites from the Sangre de Cristo and Jemez Mountains, North-central New Mexico: New Mexico Geological Society, 55th Fall Field Conference, Guidebook, p. 326-334.
Kues, B. S., and Batten, R. L., 2001, Middle Pennsylvanian gastropods from the Flechado Formation, north-central New Mexico: The Paleontological Society, Memoir 54 (supplement to Journal of Paleontology, v. 75, no. 1), 95 p.
Lucas, S. G., and Hunt, A. P., 1991, A Middle Pennsylvanian reptile from New Mexico: New Mexico Journal of Science, v. 31, p. 21-25.
Sutherland, P. K., and Harlow, F. H., 1973, Pennsylvanian brachiopods and biostratigraphy in southern Sangre de Cristo Mountains, New Mexico: New Mexico Bureau of Mines and Mineral Resources, Memoir 27, 173 p.
White, C. A., 1881, Report upon the Carboniferous invertebrate fossils of New Mexico; *in* Report upon United States geographical surveys west of the one-hundredth meridian [Wheeler Survey]: v. 3 (supplement), appendix, p. 1-38.
Young, J. A. Jr., 1942, Pennsylvanian Scaphopoda and Cephalopoda from New Mexico: Journal of Paleontology, v. 16, p. 120-125.
Young, J. A. Jr., 1945a, Paleontology and stratigraphy of the Pennsylvanian strata near Taos, New Mexico [Ph.D. dissertation]: Cambridge, Harvard University, 314 p.
Young, J. A., Jr., 1945b, *Huanghoceras bryani*, new name: Journal of Paleontology, v.19, p. 319.
Zidek, J. and Kietzke, K. K., 1993, Pre-Permian vertebrates of New Mexico, with remarks on some Early Permian specimens: New Mexico Museum of Natural History and Science, Bulletin 2, p. 1-10.

5.0 STOP 1. Flechado Formation.

[44] Pull off to right onto second paved frontage loop.

Park across from superb roadcut of nearly horizontal, shale, limestone, and sandstone beds of the Flechado Formation (Fig. 3.4). Typical marine Flechado Formation fossils are seen here. Two strands of the Pecos-Picuris fault system disrupt the strata opposite the north entrance to the pullout. Carefully cross highway to examine the rocks. **0.3**

The Flechado Formation:
First defined by Sutherland (1963), the primarily siliciclastic Flechado Formation is as much as 2500 ft thick spanning Morrowan to middle Desmoinesian time—approximately the first half of the Pennsylvanian Period. This formation is composed of sediments eroded from the San Luis-Uncompahgre uplift to the west, transported eastward by river systems, and deposited in basinal marine environments along the western side of the subsiding Taos trough. The lower (Morrowan) part of the Flechado Formation consists mainly of fine-grained siliciclastics representing strandplain, marsh, mudflat and minor stream environments of the low-lying and quiescent land mass, interbedded with shallow, marginal marine deposits. A stratigraphic section of the lower part of the Flechado Formation was measured by Sutherland and Harlow (1973) to the northwest of Stop 1 on the eastern slopes of McGaffey Ridge (on the horizon to the west, about 0.6 mile west of the Rio Grande del Rancho). During recent revisions to mapping work on the Ranchos de Taos 7.5-min. quadrangle (Bauer et al., 1999b), J. Lyman measured three sections east of the Rio Grande del Rancho (Fig. 3.5). The Great Unconformity lies along the crest of McGaffey Ridge where the steeply east-dipping Mississippian Arroyo Peñasco Group (Fig. 3.6) overlies Paleoproterozoic granite exposed on the western slope.



FIGURE 3.4. View north of roadcut through Pennsylvanian Flechado Formation at STOP 1 along NM-518. The section mainly consists of shallow marine prodelta/interdistributary bay dark gray shales and interbedded silty limestones, overlain by tan, trough-crossbedded sandstones representing distal channels of prograding fan delta lobes during a time of high discharge.

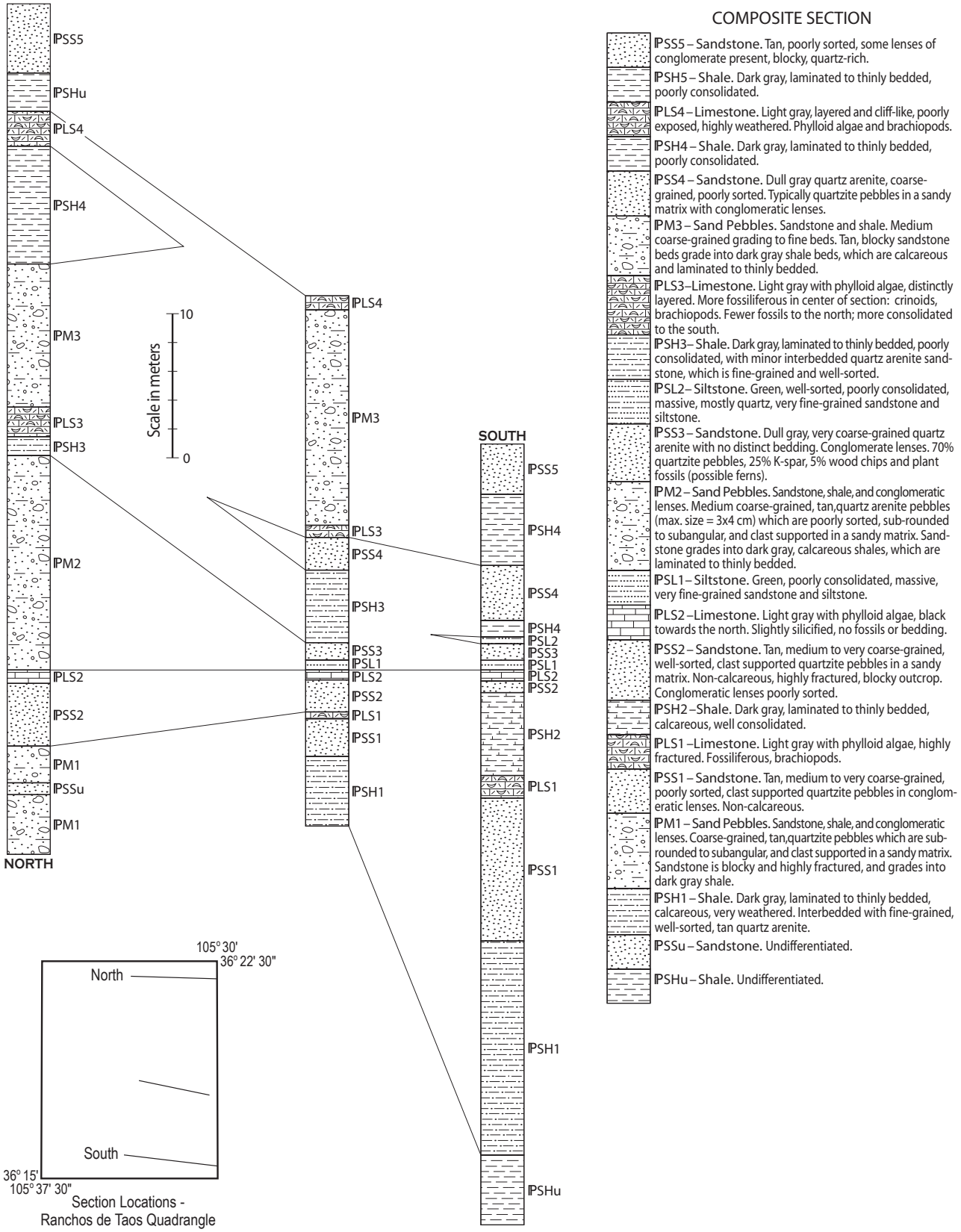


FIGURE 3.5. Composite stratigraphic sections of the Pennsylvanian rocks on the east side of the Rio Grande del Rancho in the Ranchos de Taos 7.5-minute quadrangle (Bauer et al., 1999b). The locations of the three west-east sections are shown on the index map. These columns represent the approximate thicknesses of mappable lithologic units in the hills to the east of here. Four, distinctive limestone beds were used as marker beds during the geologic mapping and are correlated in these sections. The mapping was done in 2003 by J. Lyman of New Mexico Tech and was incorporated as a revision to Bauer et al. (1999b).

Atokan and early Desmoinesian time witnessed increased tectonic activity in the Uncompahgre uplift, resulting in influx of coarser-grained clastics via alluvial fan, braided stream, and fan-delta systems, into the western margin of the Taos trough (Fig. 3.7). Progradation and shifting of fan-delta lobes across muddy shallow marine environments produced complex lateral and vertical facies changes, which were studied in detail in the Taos/Talpa area by Casey and Scott (1979) and Casey (1980a, b). According to these authors, during periods of little discharge, bed-load sediment was mainly deposited in distributary channels. During high-discharge periods, the stored sediment was entrained and fan-delta complexes prograded into shallow marine environments, resulting in coarsening-upward sandstone sequences with conspicuous, large-scale, steeply dipping delta foreset beds. Prograding into shallow marine environments, coarser-grained sediment would spread out on the delta slope, forming fan-shaped frontal splays. In cases of major and sustained sediment input, the prograding fan-deltas would be followed by braided-stream deposits and in some cases by proximal conglomeratic alluvial fan and debris-flow units in vertical succession. Such stacked sandstone/conglomerate sequences are not exposed along this stretch of highway, which mainly cuts through interlobe and prodelta marine shales and fan-delta foreset beds, but exist higher in the section, obscured by vegetation. Toward the north end of this roadcut, near the top of the exposure, is a good example of fan-delta foreset beds immediately overlying prodelta shales.

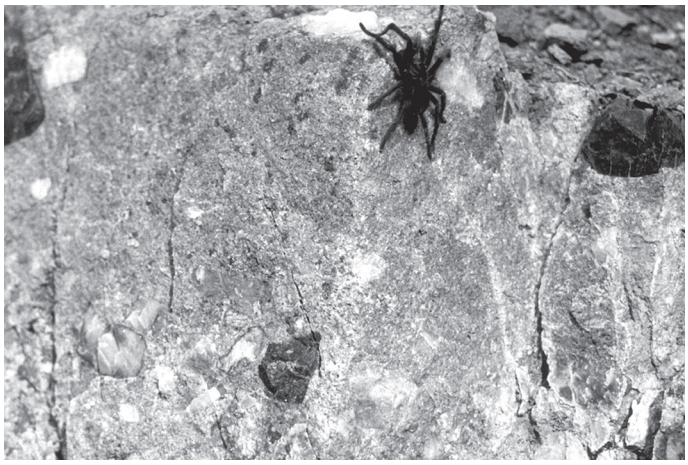


FIGURE 3.7. In the Taos area, the Pennsylvanian Flechado Formation contains rare conglomerates that contain an assemblage of robust clasts dominantly composed of various types of quartz lithologies. In this photograph, with tarantula for scale, a variety of generally well-rounded chert (dark clasts), quartzite, and vein quartz cobbles are visible.

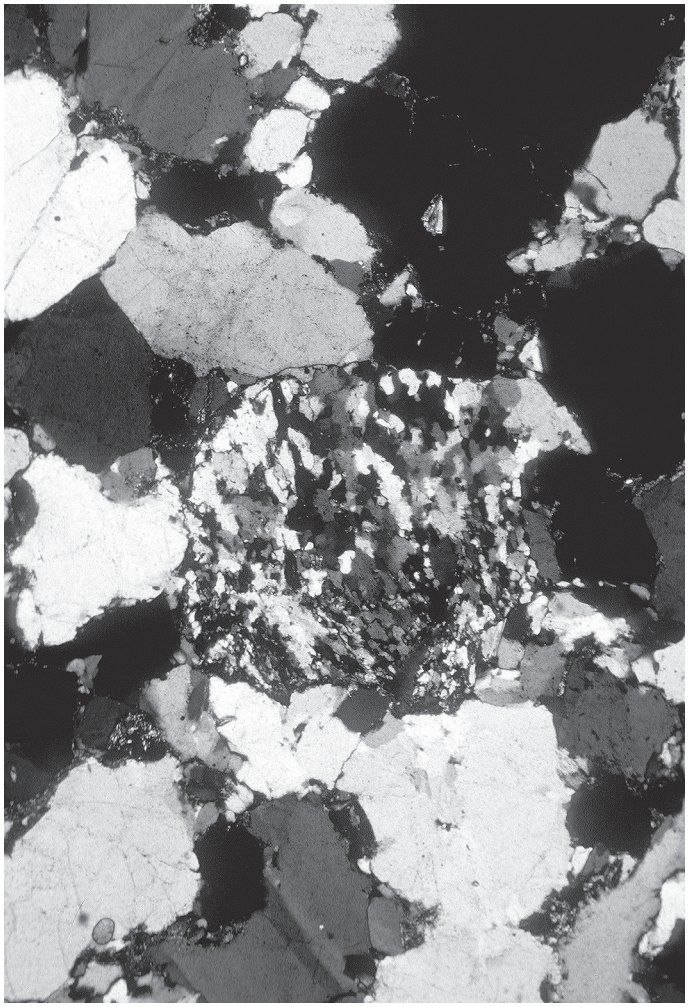


FIGURE 3.6. Photomicrograph of a thin section of the Mississippian Del Padre Sandstone Member of the Espiritu Santo Formation of the Arroyo Peñasco Group. The Del Padre Sandstone is a dense, crystalline, transgressive marine unit that can be mistaken in the field for Proterozoic quartzite. This sample is from an outcrop adjacent to the Picuris-Pecos fault southwest of here. The sandstone is seen to contain a rounded grain of Proterozoic quartz mylonite, indicating that Proterozoic highlands were being tapped in Mississippian time.

Numerous individual fan-delta lobes exist in the Taos/Talpa area, and the associated sediments preserve many of the varied depositional environments associated with deltas. For example, in some areas, plant-bearing overbank muds and sands of interdistributary upper delta flood plain and coastal plain environments are present between fluvial-deltaic deposits. In shallow marine environments, thin limestone beds (Fig. 3.8) locally developed above fan-delta lobes following delta abandonment or in interdeltaic or interdistributary embayments during periods when influx of siliciclastic sediment was minimal. Depth of the sea along the west side of the Taos trough during this time probably did not exceed 30 to 40 m.

The Picuris-Pecos Fault System:

The Picuris-Pecos fault system is the most impressive strike-slip fault system in New Mexico. It was first recognized by Montgomery (1953) in the eastern Picuris Mountains. He later mapped it southward into the southern Sangre de Cristo Mountains (Miller et al., 1963). The fault has been traced for 84 km from Taos southward to I-25 near the village of Cañoncito, and then farther south to the Lamy area. Sutherland (in Miller et al., 1963) also noted that the fault projects northward into the trace of the Sangre de Cristo fault north of Taos. Bauer and Kelson (2004a, this volume) presented a structural model for linking the two faults, and proposed that the Picuris-Pecos fault was an early rift boundary.

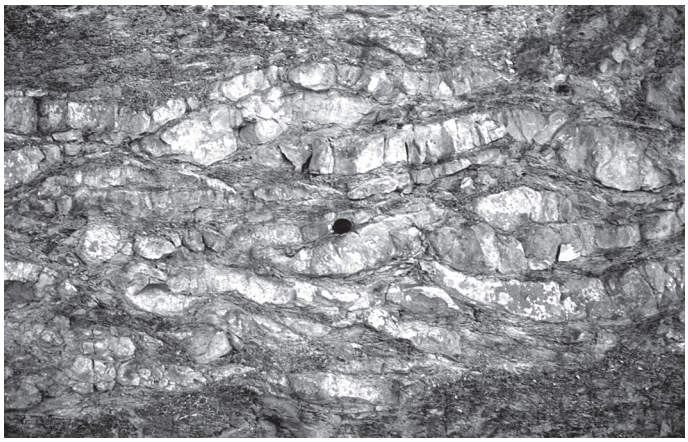


FIGURE 3.8. Soft sediment deformational features are fairly common in good exposures of Pennsylvanian rocks in the Taos trough. This photograph of interbedded sandstone and shale from a roadcut exposure south of Talpa, displays complex imbrication and folding of the sandstone layers. Camera lens cap in center of photo for scale.

Where well mapped south of Taos, the fault system consists of five, major, sub-parallel, anastomozing, near-vertical, north-striking fault zones. From west to east, they are: Picuris-Pecos, La Serna, Miranda, McGaffey, and Rio Grande del Rancho faults. The major faults are spaced 1-1.5 km apart, and are generally located in valleys due to their easily eroded fracture zones. In combination, these faults are part of a major mostly Laramide fault/fold system (Figs. 3.9 and 3.10). The high ridge at 3:00 is formed by near-vertical Mississippian rocks of the Arroyo Peñasco Group that rest above the Great Unconformity.

The Picuris-Pecos fault proper is a major crustal boundary that has experienced enough slip to juxtapose supracrustal and granitic Proterozoic rocks in the Picuris Mountains. To the south, offset Paleozoic strata indicate that the fault has a Phanerozoic east-down separation. Slickenlines typically indicate strike-slip or shallow oblique-slip on steep fault planes.

Approximately 1.3 km east of the Picuris-Pecos fault is the east-down La Serna fault, which has dropped the Picuris Formation down against the Miranda granite in the Miranda graben (McDonald and Neilsen, 2004, this volume). The west-down Miranda fault is located in Arroyo Miranda about 1.4 km east of La Serna fault. The main strand of the Miranda fault is inferred beneath Arroyo Miranda, based on water-well records and the juxtaposition of Picuris Formation and granite. Good exposures in the Talpa/Llano Quemado area, where the Miranda fault zone cuts Picuris Formation, display numerous north-striking, strike-slip faults with map separations measured on the order of meters to hundreds of meters. Importantly, the <18.6 Ma upper member of the Picuris Formation is cut by strike-slip faults within the Miranda and La Serna fault zones, suggesting that strike-slip faulting continued well into the Neogene.

Approximately 1 km east of the Miranda fault is a set of west-down branching fault splays (the McGaffey fault) located on the bedrock ridge of Cuchilla del Ojo. The McGaffey fault offsets Proterozoic and Paleozoic rocks, but appears to have considerably less throw than adjacent fault zones. Strike-slip slickenlines are common on north-striking, high-angle minor fault planes. Notably, the high-discharge Ponce de Leon warm spring is located at the intersection of the McGaffey and Embudo faults.

Approximately 1.5 km east of the McGaffey fault is the several-kilometer-wide west-down Rio Grande del Rancho fault zone, a complex family of branching faults along and east of the Rio Grande del Rancho valley. Most of the main strand of the fault zone is buried in the alluvial valley, but exposures in the Pennsylvanian rocks show extensive strike-slip breccia/fracture zones. At the northern end of the valley, Pennsylvanian bedding has been rotated into a vertical orientation against the Picuris Formation along a west-down fault. The Pennsylvanian rocks along the flanks of the Rio Grande del Rancho valley contain an abundance of outcrop-scale, Laramide-style folds and faults (Fig. 3.11).

During its long history, the fault system has accommodated both predominantly strike-slip and dip-slip movement. However, resolving the chronlology and character of the slip history along this multiply activated structure has been suprisingly difficult. Each of the fault zones probably share similar kinematic histories of multiple reactivations, as described by Bauer and Ralser (1995).

The Picuris-Pecos fault clearly displays ~40 km of dextral strike-slip map separation (Miller et al., 1963). However, that separation is based on Proterozoic-age piercing lines, and therefore only constrains the net slip for the last 1.4 Ga. Bauer and Ralser (1995) concluded that Proterozoic slip on the fault is reasonable based on ductile deflection and attenuation of strata along the fault, geometries and kinematics of Paleozoic and Laramide fault structures, the relative fracturing of Proterozoic versus Paleozoic strata, and the presence of other high-angle Proterozoic-age faults.

Sedimentological evidence exists for an active Picuris-Pecos fault in Paleozoic time. The Mississippian Del Padre Sandstone is abnormally thick at several locations along the Picuris-Pecos fault, and Sutherland (in Miller et al., 1963) concluded that they accumulated along a Picuris-Pecos fault scarp that formed through vertical movement. Additionally, Sutherland described two later episodes of west-side-up faulting along the northern exposure of the fault: in the early Pennsylvanian (Morrowan), and in the middle Pennsylvanian (late Desmoinesian).

The evidence for post-Pennsylvanian faulting is unequivocal along much of the Picuris-Pecos fault where Precambrian rocks are juxtaposed against brecciated and drag-folded Pennsylvanian strata. At least parts of the Picuris-Pecos fault were probably Paleozoic structures that were reactivated during the Laramide and again during Rio Grande rifting.

Field relations at the southernmost exposure of the Picuris-Pecos fault in the Picuris Mountains yield a constraint on the youngest faulting. The ridge north of Vadito (seen later along this route) is capped by 5.4 Ma basalt that is overlain by a quartzite-boulder gravel deposit of unknown age. Both the basalt and gravel are offset by small strands of the Picuris-Pecos fault (Bauer et al., 2003). This finding is supported by fission track work for the southernmost exposures of the fault near

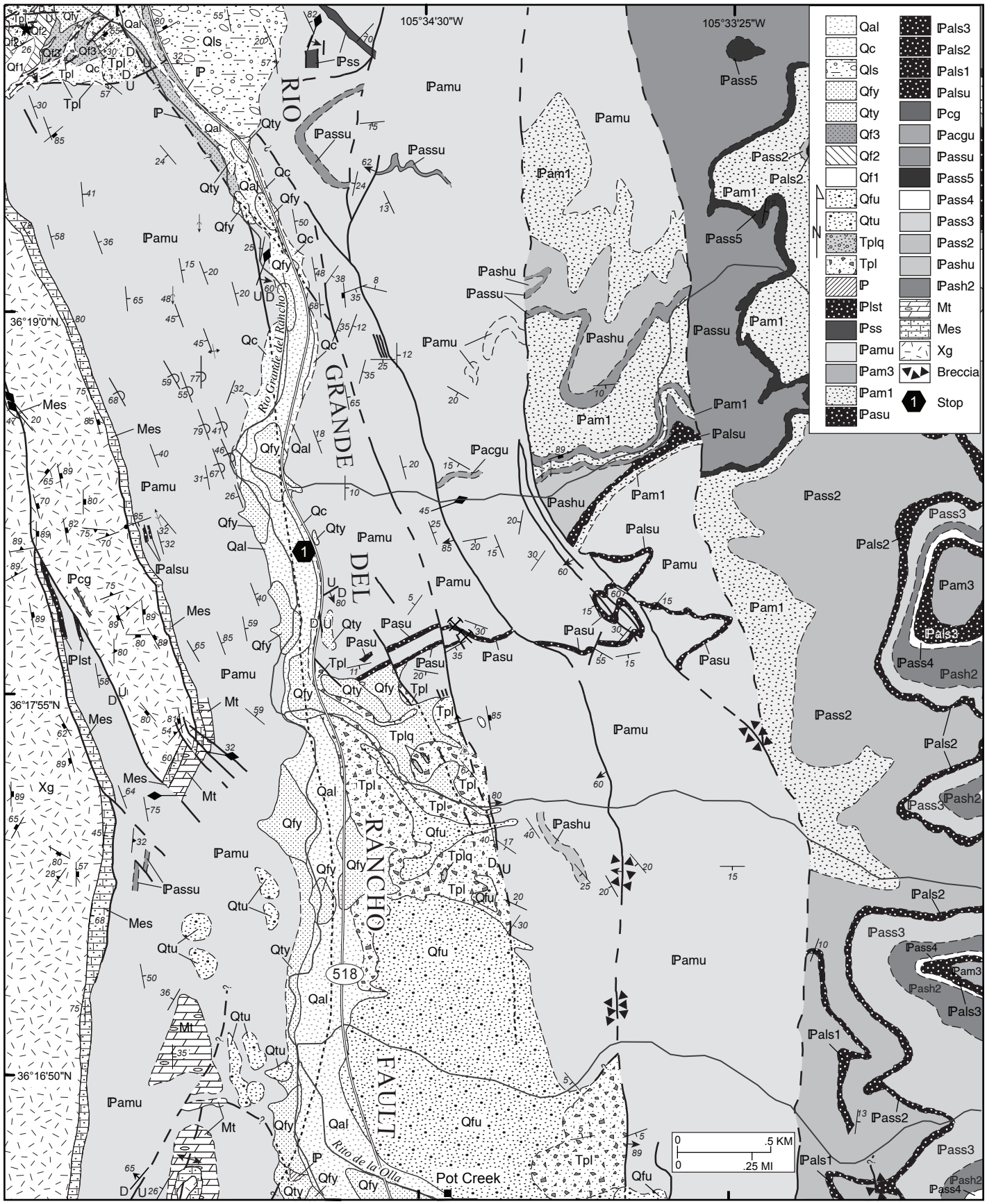


FIGURE 3.9. Geologic map of the Rio Grande del Rancho valley. Modified from the geologic map of the Ranchos de Taos quadrangle (Bauer et al., 1999).

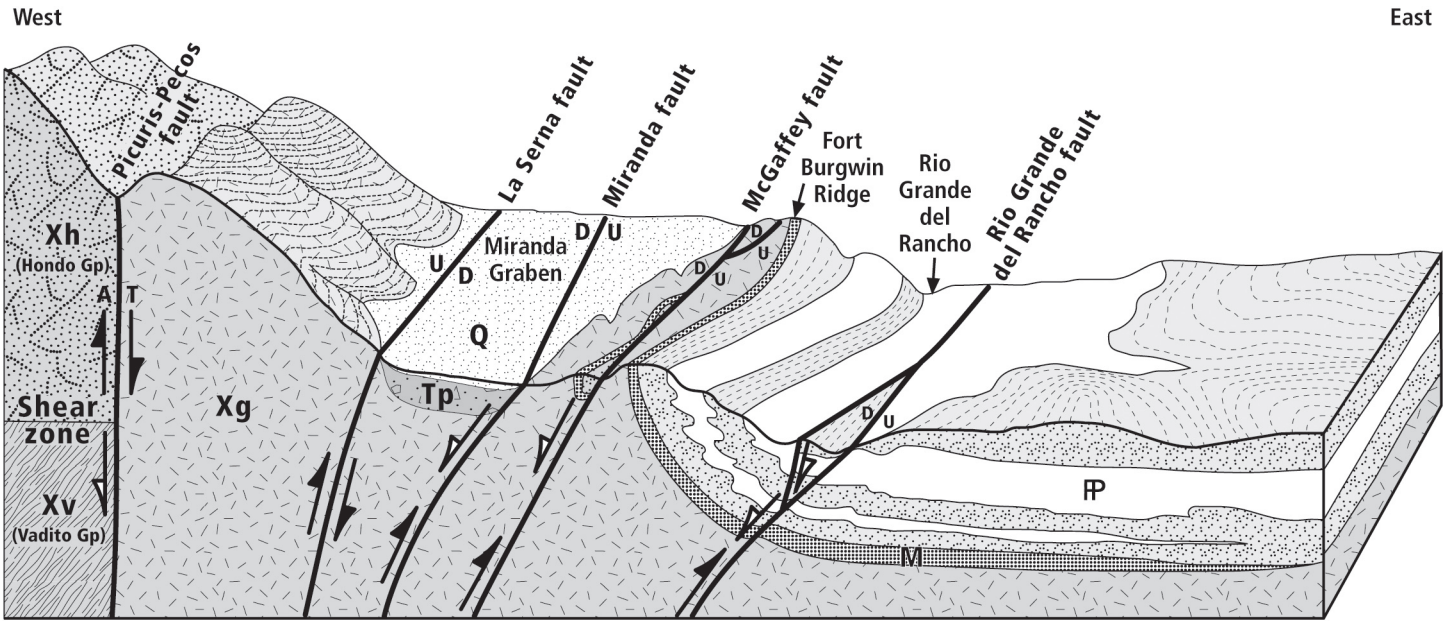


FIGURE 3.10. Conceptual structural model of the Picuris-Pecos fault system in the northeastern Picuris Mountains, modified from Chapin (1981). In this north-viewing block diagram, the principal faults are depicted as east-verging Laramide faults (solid arrows) that steepen with depth, perhaps joining at depth to form a master fault. The principal faults are interpreted as experiencing normal slip during Miocene tectonism (open arrows). The Miranda graben contains Picuris Formation overlain by thin Quaternary deposits. Q = Quaternary deposits; Tp = Picuris Formation; PP = Pennsylvanian rocks; M = Mississippian rocks; Xg = Proterozoic granite; Xh = Proterozoic Hondo Group; Xv = Proterozoic Vadito Group.

Glorieta Baldy, where Kelley (1995) concluded that throw of approximately 400 m has occurred on the Picuris-Pecos fault in the middle to late Cenozoic.

Return to vehicles and resume drive south on NM-518.

5.2 Gated Forest Service road on the left. A short hike up this road provides another exposure of the Llano Quemado breccia of the Picuris Formation, and a fascinating arroyo exposure of deformed Picuris Formation conglomerate downdropped against Pennsylvanian rocks along a major strand of the Picuris-Pecos fault system. **0.2**

5.3 On left, opposite paved pullout, is a roadcut exposure of green siltstone of the Picuris Formation. This rock is also found in the vicinity of the 35 Ma ash near Talpa (Fig. 3.2), and probably represents lower Picuris Formation deposited in the pre- to early-rift Rio Grande del Rancho graben. **0.1**

6.6 Pot Creek cultural site on left is open from late June to early September (see <http://www.fs.fed.us/r3/carson/html_main/list_pot_creek.html> for details). The nearby Pot Creek Pueblo is on the Southern Methodist University Fort Burgwin campus and is not open to the public. The pueblo probably looked similar in size and construction to Taos Pueblo today but was abandoned some 700 years ago (Fig. 3.12). Anthropologists believe that these people moved to existing settlements at Taos and Picuris Pueblos. **1.3**

6.9 Fort Burgwin Research Center on right is owned by Southern Methodist University. The center is the site of a restored cavalry post, Cantonment Burgwin (also known as Fort Fernando de Taos), was used from 1852 to 1860 and named for Captain John Henry K. Burgwin. He was killed while attacking the church at Taos Pueblo during the Taos Revolt of 1847. On March 30, 1854 near what is now Pilar, the garrison of this outpost suffered the greatest defeat for the U.S. military of that decade at the hands of the Jicarilla Apache during the Battle of Cieneguilla. Of the sixty Dragoons that fought that day only forty survived the battle and only two of those were not wounded.

The research center serves as a base for ongoing archeological studies of the Pot Creek Pueblo site by the SMU Anthropology Dept. Classes in archaeology, anthropology, biology, geology, and various fine arts are offered in three short terms during the late spring and summer months. The campus also serves as a base for geology field camps for several universities. During summer months, music and cultural events here are open to the public. **0.3**

7.1 Mile marker 66. High mesa on left (east) is capped by Pleistocene gravel. Fort Burgwin south entrance on right. Historical marker reads: *Cantonment Burgwin 1852-1860. Never officially designated a fort, this post was built to protect the Taos valley from Utes and Jicarilla Apaches. It is Named for Captain John H.A.K. Burgwin who was killed in the Taos uprising of 1847. It was abandoned in 1860, and is the site of the Fort Burgwin Research Center.* **0.2**



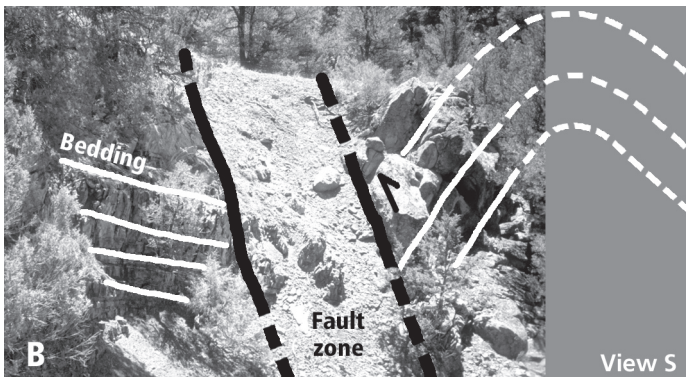


FIGURE 3.11. Good outcrop exposures of the Pennsylvanian rocks in this region are rare. It is notable that many of these rare exposures display deformational features such as reverse faults, folds, fault-bend folds, drag folds, overturned beds, and thrust faults. These structures attest to the severity and distributed nature of the Laramide tectonism in this region. Many of these structures were described by Chapin (1981) in his thesis study of the Fort Burgwin area. These two photographs, from exposures near here, show some of the outcrop-scale structural diversity of the Laramide fold/fault belt. A) View north of a west-up, high-angle fault-bend fold structure in shale. Marking pen at top for scale. B) View south of sandstone beds deflected along a meter-thick reverse fault. Footwall beds are shallowly dipping. Such structures support a kinematic model of east-directed crustal shortening during the Laramide orogeny.

7.3 Forest Road 438 on left goes several miles through the Pennsylvanian section along Rito de la Olla. Forest Road 440, just ahead on left provides access to a long dirt road loop that travels up Maestas Ridge and back down along Rio Grande del Rancho on Forest Road 439. **0.2**

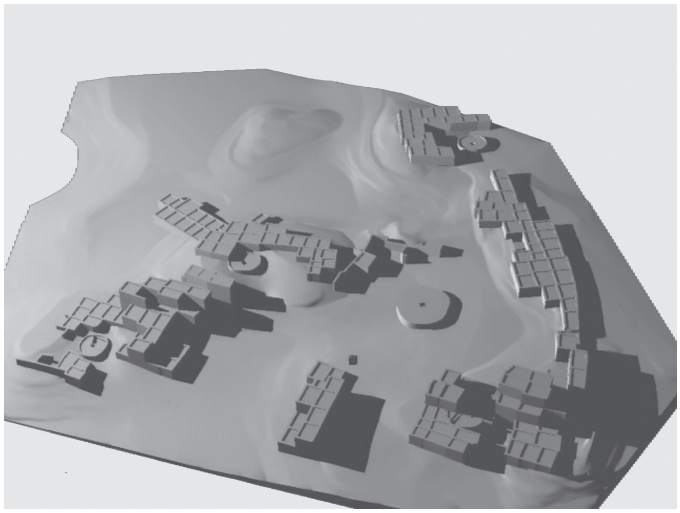


FIGURE 3.12. Pot Creek Pueblo, on the grounds of the SMU Fort Burgwin Research Center, was abandoned some 700 years ago. Between 1260 and 1320 AD, at the height of its occupation, the multistory pueblo was composed of about 400 ground-level rooms and probably looked similar to the modern Taos Pueblo. The pueblo has been, and continues to be, excavated by SMU faculty and students. Virtual reality reconstruction of the pueblo by Dennis R. Holloway, Architect (image used with permission; see <http://www.dennisrhollowayarchitect.com> for virtual reconstructions of other pueblos).

7.9 Crossing over the Rio Grande del Rancho, and beginning climb to the drainage divide at US Hill. Exposure of late Pleistocene Qt6 gravel on right (west), inset into rocks of the Picuris Formation. **0.6**

8.2 Picuris Formation conglomerates and sandstones of the lower conglomerate member are exposed in the roadcuts ahead for the next several miles. **0.3**

8.4 STOP 2. Picuris Formation conglomerate.

[45] Pull off highway into Forest Road 439 on left, park. Carefully cross highway to examine the roadcut exposure of lower conglomerate member of the Picuris Formation (Fig. 3.13). **0.2**

The conglomerate is clast-supported with well-rounded cobbles up to 40 cm in diameter. This exposure contains approximately 60% Tertiary volcanic clasts and 40% Proterozoic quartzite clasts. Volcanic clasts are predominantly andesites, accompanied by lesser volumes of basalt, basaltic andesite and dacite. Conspicuously absent are rhyolite clasts of Amalia Tuff. Basalts and basaltic andesites are typically olivine phyric, and are petrographically similar to transitional silicic alkalic basalt varieties characteristic of the early-rift volcanic sequence in the southeastern San Juan Mountains, San Luis Hills and present to lesser degrees in the Latir volcanic field (Lipman and Reed, 1989). Andesites are compositionally and petrographically variable and include porphyritic lavas dominated by pyroxene+plagioclase±hornblende phenocrysts. Dacite clasts are also compositionally and petrographically variable but are typically charac-



FIGURE 3.13. Lower conglomerate member of the Picuris Formation at STOP 2 on NM-518. The exposure along the road consists of poorly sorted, well-rounded clasts (70% Tertiary volcanic clasts of dacite, andesite, basalt, no Amalia Tuff, and 30% Proterozoic quartzite). This is the location of Rehder's (1986) measured section B, Where he interpreted 22 m of conglomerate and conglomeratic sandstone that he interpreted as debris flows related to southward-prograding alluvial fans from the Latir volcanic field.

terized by moderate amounts of hornblende+plagioclase±biotite phenocrysts. Compositionally similar volcanic sequences are present in the pre-caldera section of the Latir volcanic field and are a regionally significant component of pre-rift Tertiary volcanism of southern Colorado and northern New Mexico. The Proterozoic clasts are mostly aluminous quartzite containing kyanite and sillimanite, identical to the Ortega Formation in the Picuris, Taos, and Tusas Mountains. These rocks were the subject of Rehder's (1986) measured section 'B', which consists of 22 m of mostly conglomerate and conglomeratic sandstone. Rehder (1986) interpreted some of the conglomerates as debris flows associated with alluvial fans that prograded southward-from the Taos Range and Latir volcanic center.

Due to the extensive local faulting and poor bedrock exposure, we are unsure of the precision of Rehder's (1986) stratigraphic reconstruction in this area. Near the base of the outcrop (as shown on section 'B' of Rehder, 1986) is a 2-m-thick, yellowish gray to light olive brown, and well-sorted ash bed that contains altered biotite crystals and few lithics. He interpreted this deposit as a primary ash fall. Below the ash is a meter-thick sandstone containing root casts. Our recent attempt to date the ash using the $^{40}Ar/^{39}Ar$ method was unsuccessful due to a lack of suitable material for analysis. However, in support of his stratigraphic interpretation, we have mapped a similar ash in Arroyo Miranda ($^{40}Ar/^{39}Ar$ date of 27.93 ± 0.08 Ma) in close proximity to the Llano Quemado breccia ($^{40}Ar/^{39}Ar$ date of 28.35 ± 0.11 Ma—see Table 2.1 in the Day 2 road log).

Return to vehicles and continue south on NM-518.

As we follow NM-518, we leave the banks of the Rio Grande del Rancho and follow Ojo Sarco Canyon for the next mile. We then depart Ojo Sarco Canyon and cross a series of drainages until we reach the pass at U.S. Hill. From Ojo Sarco Canyon to U.S. Hill we will be cutting across the structural grain of the Picuris-Pecos fault system, and will notice abrupt changes in dip and rock types over short distances.

9.2 Forest Service Road 476 on right leads to Vallecitos, although no overt evidence remains of its human habitation. **0.8**

9.6 More Picuris Formation lower conglomerate member is exposed in the roadcut on the right. **0.4**

10.2 The Ojo Sarco drainage ahead on right probably contains a fault that separates the Picuris Formation to the west from Pennsylvanian strata to the east. The area ahead has not been mapped in detail, although the abrupt changes in lithology in the roadcuts (from Picuris Formation to Pennsylvanian rocks to Proterozoic granite) indicate that we are driving across strands of the Picuris-Pecos fault system. **0.6**

11.6 Carbonaceous Pennsylvanian shale crops out in the roadcut on the right. **1.4**

12.5 Scenic pullout on left, just before U.S. Hill. At this elevation (8600 ft) we are in the uppermost part of the mixed conifer woodland vegetative zone dominated by Douglas fir, white fir, ponderosa pine, and aspen. A few hundred feet higher is the spruce-fir woodland zone composed of Engelmann spruce, sub-alpine fir, limber pine, blue spruce, aspen, and some Douglas and white fir. **0.9**

12.6 This divide has been called U.S. Hill since the U.S. Army first built the road in 1854, that made travel and communication possible between Fort Union, Cantonment Burgwin, and settlements in southern Colorado.

U.S. Hill marks the drainage divide between water that flows northward into the San Luis Basin and water that flows southward into the Española Basin. However, exotic cobbles observed on this topographic saddle suggest a paleotopography that must have differed appreciably from the modern landscape.

We are near the east edge of the 8-km-wide Picuris-Pecos fault system. The Picuris-Pecos fault proper is about 5 km west of here, but between here and there are the southern extensions of La Serna, Miranda, and Rio Grande del Rancho faults.

Forest Road 114 on the right leads to the fire lookout tower on Picuris Peak (10,801 ft). Picuris Peak is formed of a highly resistant strike ridge of Ortega Formation quartzite along the southern limb of the Hondo syncline, an early Proterozoic structure that underlies most of the Picuris Mountains. Forest Road 442, on the left, forms a torturous loop (Fig. 3.14) that joins Forest Road 439 near the headwaters of the Rio Grande del Rancho. **0.1**

14.5 [46] For OPTIONAL STOP 3, turn right onto the gravel road that leads to the mica mine (*mileage to the mine is not included in this log—0.8 miles each-way*). **1.9**

OPTIONAL STOP 3. Oglebay Norton Mica Mine. [47]

This is the only major mica mine west of the Appalachian Mountains. Prior to visiting the mine, contact the property owner for permission.

As this road log is being written, the future of mining here is uncertain. The mine is for sale by the current owners, who have filed for Chapter 11 bankruptcy protection. In addition, Picuris Pueblo has filed suit claiming aboriginal title to the land.

The open pit operation (Figs. 3.15 and 3.16) is developed in Paleoproterozoic feldspathic, quartz-eye, muscovite schist that was mapped as Rio Pueblo schist by Montgomery (1953) and Bauer (1988). The Rio Pueblo schist crops out in a number of small exposures east of the Picuris-Pecos fault. These rocks were interpreted as altered felsic metavolcanic rocks (Bauer, 1988), perhaps equivalent to the upper feldspathic section of the Vadito Group such as is exposed in the Pilar cliffs. A sample of Rio Pueblo schist from near Comales Campground southeast of here, yielded a preliminary U/Pb-zircon age of approximately 1680 Ma (S. Bowring, personal commun., 1996). The hills of



FIGURE 3.15. Digital orthophotograph from an image taken in 1997 of the mica mine area, eastern Picuris Mountains.



FIGURE 3.14. Field work in the transcendent Picuris Mountains can require field skills other than geologic mapping. In this 1982 photo, UNM Professor J.F. Callender clears trail while his graduate student heroically shoots photos.

Rio Pueblo schist in the mine area may represent original erosional highlands that were onlapped by Mississippian and Pennsylvanian sediments, and later modified by faults.

Picuris Pueblo clay and pottery:
Micaceous clays, used to make micaceous pottery, are known to exist in many areas in north-central New Mexico. Most commonly, they developed during the weathering of Proterozoic mica-bearing pegmatites and schists. Many pegmatites were mined for sheet and flake (or scrap) mica starting in the 18th century, reaching a peak before World War II, but ending in the early 1960s. Of the 14 known occurrences in the archives of New Mexico Bureau of Geology and Mineral Resources, most are related to the mica-bearing pegmatite mines and are on U.S. Forest Service land. Two occurrences are on federal land administered by the U.S. Bureau of Land Management, one is on state

COMMERCIAL MUSCOVITE FROM THE U.S. HILL MINE, PICURIS MOUNTAINS, TAOS COUNTY, NEW MEXICO

James M. Barker [1], Ken Santini [2], and George S. Austin [1]

[1]New Mexico Bureau of Geology and Mineral Resources, New Mexico Institute of Mining and Technology, Socorro, New Mexico 87801;
[2]Santini and Associates, Oro Valley, Arizona, 85737

Muscovite mica is produced by Oglebay Norton at their U.S. Hill Mine in the Peñasco Mining District of the Picuris Mountains in Taos County, north-central New Mexico (Austin, Barker, and Bauer, 1990). Mineral Industrial Commodities of America first mined this deposit in 1959. They built a new processing plant at Velarde in the early 1980s and added a flotation circuit in 1984 (Nelson, 1996). Franklin Industrial Minerals bought the operation in July 1990 and sold it to Oglebay Norton in 1999. The mine is currently operating, but Oglebay Norton filed for Chapter 11 bankruptcy on February 23, 2004 (Industrial Minerals, 2004). The Picuris Pueblo filed an aboriginal title claim in state District Court in Taos against Oglebay Norton regarding the mine area on February 20, 2004. The pueblo claims that the land is sacred to them and that traditional collection sites for micaceous clay, essential to distinctive Picuris pottery, have been or will be desecrated by mining. The operation is now for sale, along with Oglebay Norton's King's Mountain mica operation in North Carolina, and is undergoing due diligence by potential buyers.

The U.S. Hill mine is about 3 km northeast of Rio Pueblo on 10 patented claims comprising 194.65 acres and an additional 12 unpatented claims within the Carson National Forest. These are in sections 23 to 25, T23N, R12E and sections 19 and 30, T23N, R13E on the Tres Ritos 7.5-minute quadrangle in the Carson National Forest at an elevation of about 8600 ft. The U.S. Hill Mine is the only mica producer west of the Mississippi, and one of nine in the U.S. Domestic production was 98,000 mt in 2003 and the average price was $120 per mt.

Perfect basal cleavage allows muscovite to be split into thin sheets that are reflective, refractive, chemically inert, insulating, lightweight, hydrophilic, flexible, elastic, and tough. It decomposes only in hydrofluoric acid and has low electrical conductivity and high dielectric strength and dielectric constant. Mica also is stable when exposed to electricity, light, moisture, and extreme temperatures. These characteristics give mica many commercial applications. The number of mica end uses is increasing, due, in large part, to surface treatment. The flake mica produced by Oglebay Norton at Velarde is used primarily as an additive to control shrinkage and increase workability in joint compound for drywall installation. It is also used as a functional filler in plastics, paint, and rubber and as an oil-well sealant.

Geology

The U.S. Hill mine is on the south side of a hill where outcrops of Proterozoic muscovite schist are surrounded by Paleozoic rocks. The muscovite schist at the U.S. Hill mine is in the Rio Pueblo schist within the uppermost Vadito Group (about 1700 Ma old) that represents a succession of metamorphosed bimodal volcanic rocks and immature sedimentary rocks. The Vadito Group is overlain by the more mature metasediments of the Hondo Group, which includes the 1-km-thick quartzite of the Ortega Formation (Bauer, 1984, Bauer, 1988, Bauer and Williams, 1989). The muscovite schist being mined is a felsic metavolcanic rock (Bauer, 1988) altered by intense deformation and recrystallization along the contact with the overlying quartzite (Beckman, 1982). The strike of the muscovite schist is northwest-southeast and typically displays at least one dominant foliation and a well-developed down-dip extension lineation. Parallel or subparallel compositional layering and the dominant foliation in the muscovite schist generally dip about 45 to 55° south.

Muscovite-Rich Zone

The mica at the U.S. Hill mine is sodium muscovite (paragonite), based on x-ray diffraction analysis, rather than sericite as is sometimes stated. The original operators received a preferential shipping rate for sericite over muscovite so they chose to call the mica "sericite." Beckman (1975) called the fine-grained mica "sericite" on textural grounds in hand specimens, trenches and 18 drill holes.

The following discussion of ore body lithology is derived mainly from Beckman (1975): Green chlorite is rare, microcline comprises up to 15%, and quartzite interbeds occur in the muscovite ore body. Five rock types exist at the U.S. Hill mine:

1. "Sericite"—Ranges from 40 to 70% mica, green-gray, very soft, crumbly; contains bouldery vein quartz, local iron oxide stain, and black magnetite and/or illmenite specks on mica flakes.

2. "Sericite" schist—Ranges from 20 to 40% mica, green-gray to gray-brown, moderately soft but competent, thin mica laminae



FIGURE 3.16. View northwest of the mica mine open pit in 1999. Mining proceeded northwest along strike of the southwest-dipping Proterozoic schist. The proximity of this mining operation to the Pueblo of Picuris and the destruction of some traditional micaceous clay deposits used for Pueblo pottery have resulted in much animosity.

between and along quartz grains; iron staining, if present, due to oxidation of black magnetite and/or illmenite specks and/or red garnets.

3. "Sericite"-quartz schist—Ranges from 20 to 30% mica, gray-brown, moderately hard, thinly laminated; generally more iron staining due to the presence of garnets; black magnetite and/or illmenite specks common; wavy quartz blebs and stringers common.

4. Micaceous quartzite—Ranges from 10 to 20% mica, gray-brown to blue-gray, hard, medium-grained with sandy texture, thin micaceous partings rare, with well-cemented quartz; some specks of black magnetite and/or ilmenite and rare garnet.

5. Quartzite—Ranges from 2 to 10% mica, gray-brown to gray-blue, very hard, dense, medium- to coarse-grained, fractures are common and often filled with calcite; typical rock above and below the ore body.

The muscovite ore body at the original pit contained two zones. The lower, higher-grade zone consisted of 2 to 18 m of 40 to 70% muscovite. This lower zone pinched out at the east and west ends of the ore body in 1975. The upper, lower-grade zone contains all five rock types listed above, some of which are too muscovite-poor to make grade. This upper unit averages about 25% muscovite in the 45 to 60 m mined. The combination of the upper and lower zones has an average muscovite grade of about 33% over the mined thickness of 47 to 78 m.

A north-trending fault truncates the ore zone on the east side of the mine. Other north trending faults cut the ore body. The relationship between the ore body and the Paleozoic rocks to the west is unclear so the extension of the orebody and potential reserves in this direction is not precisely known. Early estimates based on 18 drill holes placed reserves at about 2,450,000 mt at a stripping ratio of 1.10:1.00 with about 820,000 mt of recoverable muscovite (Beckman, 1975). Economic muscovite at that time was any material with 25% or more +200 mesh mica.

Mining and Milling of Mica

Muscovite schist at the U.S. Hill mine is ripped or bladed by D-9 bulldozers, pushed into blended stockpiles, and moved by front-end loader to the onsite screening plant. The schist averages approximately 40% muscovite before it is passed over a 10-cm grizzly. The <10 cm fraction is crushed to <1.9 cm and passed through a double screen. The >1.9 cm fraction averages 25 to 35% muscovite and is stockpiled. The <1.9 cm fraction averages approximately 60% muscovite and is trucked by contractors 50 km to the mill just south of Velarde on NM-68 and about 55 km north of Sante Fe.

Muscovite conveyed to the flotation mill is pulverized in a rod mill at a charge of 25 to 35% and classified on screens with the <230-mesh fraction reporting to slimes. The flotation feed is diluted, pH adjusted with sulfuric acid, and an amine collector is added to the rougher cells. Rougher concentrate reports to the cleaner stage, is dewatered and conveyed to the fluid-bed steam-tube dryer (<160°C) circuit. The dried muscovite is sent to the grinding circuit where it is reduced in size and delaminated by cool, dry, opposing muscovite-laden air-streams in a fluid-energy mill. The finished muscovite product is air-sorted and placed in bags or supersacks for shipment by truck. Containers may be shipped by rail to ports for overseas customers (Nelson, 1996). Finished muscovite ranges in size from 1 to 100 µm and is very white with a brightness of 80 to 90% (over 90% when bleached).

Tails from prior mining and milling contain 35% muscovite but are not now processed. Tailings from the flotation circuit consist mainly of ground and washed quartz with some large mica flakes that may later be reclaimed. They are dewatered and stored near the plant along with tailings from the dry-grind circuit.

REFERENCES

Austin, G. S., Barker, J. M., and Bauer, P. W., 1990, Precambrian muscovite from the M.I.C.A. mine, Picuris Mountains, New Mexico: New Mexico Geological Society, 41st Fall Field Conference, Guidebook, p. 369–374.

Bauer, P. W., 1984, Stratigraphic summary and structural problems of Precambrian rocks, Picuris Range, New Mexico: New Mexico Geological Society, 35th Fall Field Conference, Guidebook, pp. 199–204.

Bauer, P. W., 1988, Precambrian geology of the Picuris Range, north-central New Mexico: New Mexico Bureau of Mines and Mineral Resources, Open-file Report 325, 259 p.

Bauer, P. W. and Williams, M. L., 1989, Stratigraphic nomenclature of Proterozoic rocks, northern New Mexico—revisions, redefinitions, and formalization: New Mexico Geology, v. 11, p. 45–52.

Beckman, R. J., 1975, Exploration and testing of the Taos mica deposit: Unpublished report, U.S. Forest Service, Santa Fe, New Mexico, 51 p.

Beckman, R. J., 1982, Mica resources of the western United States: New Mexico Bureau of Mines and Mineral Resources, Circular 182, p. 35–37.

Industrial Minerals, 2004, Oglebay goes Chapter 11: Industrial Minerals, No. 439, April, p. 8.

Nelson, G. L., 1996, Franklin Industrial Minerals—Mica plant operations in New Mexico: New Mexico Bureau of Mines and Mineral Resources, Bulletin 154, p. 159–164.

land, and one is on a patented claim. These clays are commonly red to dark brown, but a few are buff colored.

Minerals present in samples from these localities are dominantly quartz, feldspar, and clay. Muscovite, a relatively resistant mineral and the one that produces the distinctive sheen on local pottery, is present in all size ranges from the finest to coarsest fractions. Clay-size mineral analyses were performed on all but one of these samples. Although kaolinite is present from trace amounts to as much as three parts in ten, the clay minerals present are dominantly illite, calcium smectite, and illite-smectite mixed-layer (I/S) clay minerals. This is not surprising since kaolinite results from intense leaching, which was not common in New Mexico's geologically recent past. In the present climate, feldspars and ferromagnesian minerals weather to form smectite, I/S, and illite. The red and brown colors in the majority of clay occurrences result from the weathering of

iron-bearing minerals. Where the original iron-rich minerals are sulfides, the leaching was perhaps intense enough to produce kaolinite.

In the 14 samples analyzed (two samples came from one of the occurrences), clay-size grains vary from a high of 36% to a low of 8%. Sand-size grains vary from a high of 57% to a low of 2%, while silt-size grains commonly are dominant in nearly all of the samples.

In preparing micaceous clays similar to these for use as pottery material, coarser particles are separated by screening. In some cases, the clay is upgraded by flotation. However, an effort is made to retain muscovite, which is commonly present as silt- or even sand-size flakes.

Micaceous pottery, while often very attractive, has typically been used for utilitarian purposes. The mica makes the vessels exceptionally strong and they are often used for cooking. Even today, many locals use these pots on modern stovetops. They claim that beans taste much better when cooked this way.

Industrial Uses of Mica:
1. Joint Compound: Joint compound is the latex-based paste used to fill the joints in gypsum dry wall. Mica prevents cracking of the large seams and makes the compound easier to apply.
2. Paint/Coatings: Mica provides durability and helps coatings to resist cracking and checking. It promotes wet adhesion, provides UV resistance, and reduces moisture vapor transmission.
3. Adhesives/Sealants: Small amounts of mica are used in adhesives and sealants to reduce shrinkage and cracking.
4. Foundry coatings: Mica is used in coatings for die-castings and in sand molds to prevent casting defects. Mica allows gas to escape and insulates the mold, enabling the metal to completely fill the mold before hardening.
5. Thermoplastic resin composites: Mica is used to reinforce polypropylene, high-density polyethylene, thermoplastic olefin blends, and engineered plastics. Mica increases stiffness and prevents parts from warping when they are taken from the mold. Mica also provides decreased shrinkage and lowers the coefficient of thermal expansion of parts, improving dimensional stability during temperature fluctuations.
6. Phenolic resin composites: Mica is used in phenolic resin composites to increase dielectric properties, as mica does not conduct electricity and is used as an insulator.
7. Rubber roofing: During preparation of rolled rubber roofing, mica is dusted on the surface to improve venting of gases during vulcanization. It also reduces sticking of the roll layers.
8. Sound deadening: Mica is used to enhance soundproofing in auto floor and firewall mats. It is also used in sound partitions.
9. Stucco: Mica is used in stucco to reduce cracking and moisture vapor transmission, and provide UV protection.
10. Electrode coatings: Coated electrodes are used where alternating current is employed for welding. Mica in the coating stabilizes the arc and protects the weld from oxygen. It accomplishes this by regulating the slag flow and gas formation during the welding process.
11. Fire extinguisher formulations: Mica is used to keep the powder in dry fire extinguishers free flowing. It keeps the powder mixture from packing tightly in the canister.
12. Gaskets: Mica provides creep resistance, reduces shrinkage, and increases resistance to swelling caused by organic liquids.
13. Brake pads: Mica is used in brake pads mainly due to its heat resistance. It reduces the flow of heat (insulates) and helps keep brake drums cool.

Return to vehicles, backtrack, and continue south on NM-518

*(note the 1.6 mile roundtrip detour to OPTIONAL STOP 3 is not included in the log mileage)***.**

15.1 The high mesas on both sides of the road are capped by erosional remnants of vesicular basalt flows. A sample from this area yielded a $^{40}Ar/^{39}Ar$ age of 5.44 ± 0.20 Ma; a second sample from the westernmost exposure of the flow, near Picuris Pueblo, was dated at 5.67 ± 0.12 Ma (Aby et al., 2004, this volume). These ages pre-date Servilleta Basalt eruptions and suggest these remnants reflect the distal margins of outflow from basaltic centers of the Ocate volcanic field to the east. The Ocate volcanic field erupted a compositionally variable suite of predominantly basaltic lavas between 6 Ma and 5 Ma (Aubele and Crumpler, 2001). Recent geologic mapping in the Peñasco quadrangle has defined a several-km-long zone of scattered exposures of basalt from the west edge of the mesa to Picuris Pueblo (Bauer et al., 2003). In general, these basalt remnants appear to be down-dropped westward along north-striking, high-angle Picuris-Pecos faults. A quartzite gravel deposit that is locally offset by north-striking faults overlies the basalt-capped high mesa west of the road. The age of the high gravel is unknown (Pliocene to early Pleistocene?), but its field relations indicate that the youngest motion on the Picuris-Pecos fault system is less than about 5.5 m.y., and possibly considerably younger. **0.6**

15.3 High roadcut on left consists of tan and yellow silt stones, sandstones, and gravels of the Picuris Formation. **0.2**

15.6 On the left, as the road bends left, opposite the turnout on the right, is a spectacular roadcut exposure (Fig. 3.17) of the middle tuffaceous member of the Picuris Formation (Aby et al., 2004, this volume). These volcaniclastic sedimentary rocks are tentatively correlated with exposed sections on Cerro Blanco near Vadito (the site of STOP 4) and 'Hill 7751' west of Picuris Pueblo. This outcrop also contains high-angle faults in its south end. Tuffaceous Picuris Formation sediments are underlain here by a thick section of the lower conglomerate member (Aby et al., 2004, this volume) of the Picuris Formation, which in turn overlie Paleozoic sedimentary rocks. These outcrops were specifically mentioned by Cabot (1938) when he originally defined the Picuris Tuff. **0.3**

16.1 [48] **Intersection with NM-75. Turn right onto NM-75 towards Vadito and Peñasco.** NM-518 heads eastward over the Sangre de Cristo Mountains past Sipapu ski area, Tres Ritos, Holman, Mora, and into Las Vegas, New Mexico.



FIGURE 3.17. Panoramic photo of Picuris Formation roadcut on NM-518 at Mile 16.1, with the Bauer quintuplets for scale. This spectacular exposure of southwest-dipping middle tuffaceous member is probably equivalent to the fine-grained middle member exposed on Cerro Blanco at STOP 4. Several faults cut the outcrop, but this area has not yet been mapped in detail.

The high wall on the left contains a splendid exposure of the contact between the lower conglomerate member of the Picuris Formation and west-dipping Pennsylvanian strata (Fig. 3.18). Over the next several miles are roadcut exposures of the Picuris Formation on the right. Although these strata generally dip southerly, parts of the slope to the north are mapped as landslides (Bauer et al., 2003). Small, north-striking, Picuris-Pecos faults cut the Picuris Formation throughout this zone, and larger faults are inferred in some of the covered valleys. **0.5**

16.7 Pliocene basalt flows are visible along the skyline at 12:00 high. **0.6**

17.4 Entering the village of Placita (also known as Rio Pueblo). The Rio Pueblo (river) heads in the Sangre de Cristo Mountains near Tres Ritos, and merges with the Rio Santa Barbara to become Embudo Creek, which joins the Rio Grande near Dixon (Fig. 3.19). **0.7**



FIGURE 3.18. The "Rock Wall" at the intersection of NM-518 and NM-75. This magnificent roadcut displays the only known exposure of the unconformable base of the Picuris Formation. In the photo, the very coarse-grained lower conglomeratic member of the Picuris Formation (light-colored boulder deposit on left) overlies west-dipping Pennsylvanian strata (dark-colored strata on right) along a 20° west-dipping angular unconformity. Note the large boulders of Proterozoic quartzite and granite in the basal Picuris Formation.

17.5 The canyon on the right exposes a ledgy, pumice-bearing section of the middle tuffaceous member of the Picuris Formation. Measured section 'H' of Rehder (1986), consists of 83 m of well-bedded sandstone that contains abundant clasts of pumice, moderate silicic volcanic clasts, rare intermediate volcanic clasts, Amalia Tuff clasts only in the uppermost 10 m, and no Precambrian clasts. Rehder (1986) assigned the section to his upper member, correlative with sandstones in Miranda Canyon. However, Bauer et al. (2003) correlated this section with excellent exposures on the tops of Cerro Blanco and Hill 7751 west of here, and Aby et al. (2004, this volume) assigned them all to the middle tuffaceous member of the Picuris Formation. Recent geologic mapping identified faults in this canyon, casting some doubt on the thicknesses reported for the measured section. **0.1**

17.7 A series of fluvial terraces along far side of the Rio Pueblo reflects the complex, Pleistocene geomorphic history of this stream. **0.2**

18.6 Mile marker 18. **0.9**

18.9 Entering Picuris Pueblo Reservation. **Any geologic investigations on tribal lands must first be approved by the tribal government.** **0.3**

19.1 **Just after large open storage shed and "tractor** **[49]** **crossing" sign, turn right** onto unmarked dirt road into Telephone Canyon. If you reach the village of Vadito, you have passed the turn. **0.2**

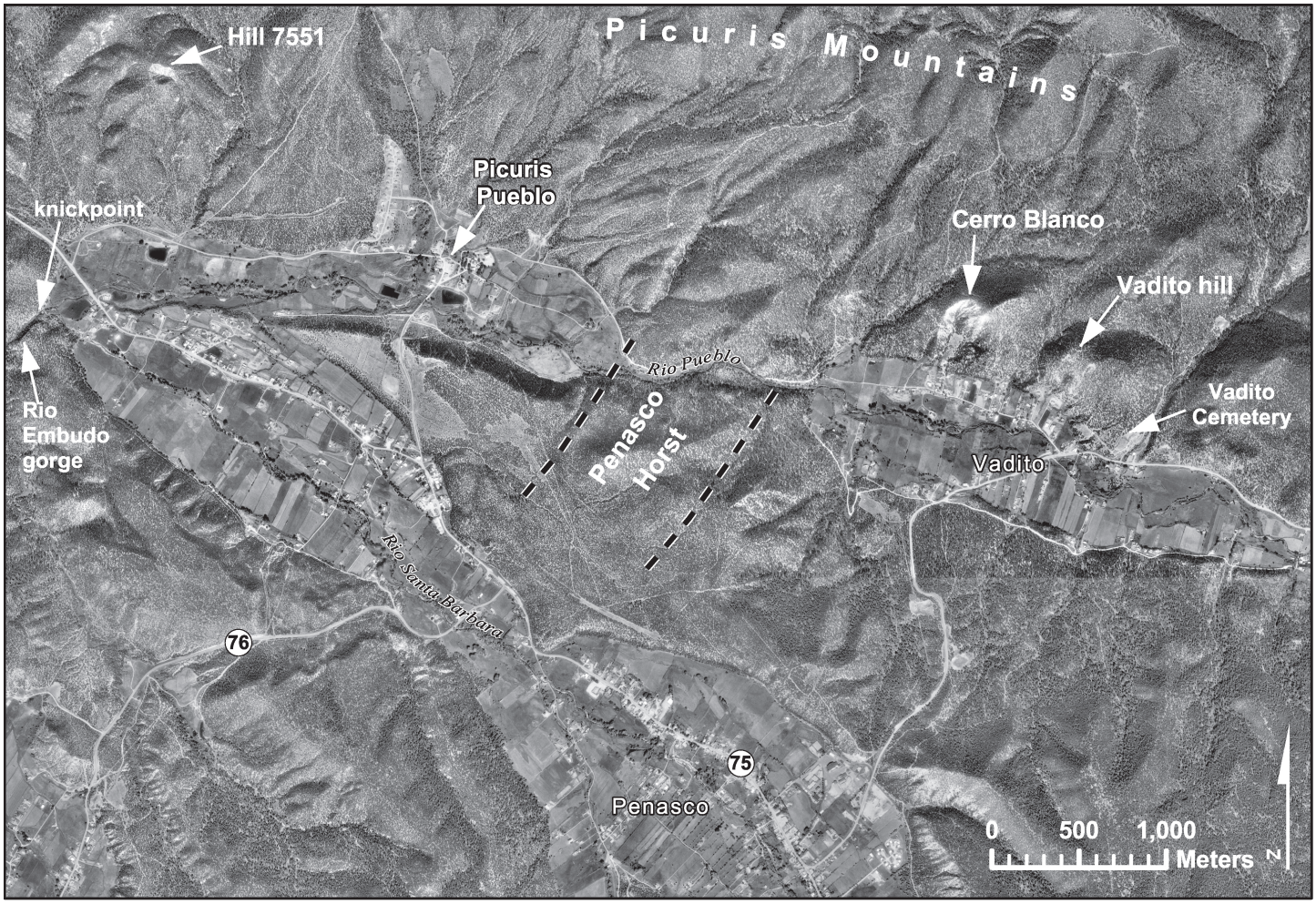


FIGURE 3.19. Aerial orthophotograph of the principal area of exposure of the Picuris Formation south of the Picuris Mountains. Three hills along the southern flank of the Picuris Mountains 'Hill 7751,' Cerro Blanco, 'Vadito hill') provide spectacular exposures of the middle and upper members of the Picuris Formation (Aby et al., 2004, this volume). Although numerous north-striking, high-angle faults of the Picuris-Pecos fault system have been mapped in the southern Picuris Mountains (Bauer et al., 2003), the range front appears to lack an east-striking master fault. This image nicely displays the dramatic fluvial geomorphology of the Rio Pueblo/Rio Santa Barbara/Rio Embudo drainage system. A lower knickpoint has formed where the pastoral Rio Pueblo and Rio Santa Barbara join and plunge into the steep-walled, high-gradient Rio Embudo canyon. Upstream, the Rio Pueblo is superimposed on the Peñasco horst and similarly changes from a meandering stream in a wide Quaternary floodplain to a narrow bedrock canyon.

19.2 Small gravel borrow pit on the left is developed in Qfo (old alluvial fan deposits). **0.1**

19.3 **Turn left sharply up rough dirt road** that climbs
[50] **towards the Vadito Cemetery.** **0.1**

19.5 STOP 4. Picuris Formation at Vadito Hill and Cerro Blanco
[51]

Park in cemetery parking lot. ***WARNING: This stop is on land owned by the Pueblo of Picuris. ACCESS IS BY PERMISSION ONLY. Under no circumstances should anyone cross on to tribal lands without permission from the tribal government.*** We will hike westward from the cemetery to Vadito Hill and Cerro Blanco for an examination of the Picuris Formation and overviews of the Española Basin and Picuris Mountains (Fig. 3.19). **0.2**

Stratigraphy and geochronology of the Picuris Formation in the Peñasco area:
There is considerable lateral variation in the Picuris Formation in this area. In general, the middle tuffaceous member consists of a lower, fine-grained, massive-to-tabular section containing rare primary ash-fall beds. Upwards in this tuffaceous section, beds of basement-derived clasts generally become more common (particularly to the west). Pumice is also generally more common and coarser upward in the section. Above the massive-to-tabular tuffaceous section lie pumice and/or Tertiary volcanic clasts and/or Proterozoic clast-rich conglomerates that are commonly silica-cemented (Fig. 3.20). Pumice clasts from this section yield dates of ~23.0 Ma (Cerro Blanco) and ~27.7 Ma ('Vadito Hill'). This range of dates indicates either mixing of clasts of various ages during transport or fault offset between Cerro Blanco and Vadito hill. North-striking, high-angle faults of the Picuris-Pecos fault system are common in this area, and have produced an overall west-down stepping of Picuris Formation and younger units including the ~5.6 Ma basalt and an overlying gravel deposit (Fig. 3.21). Cerro Blanco is capped by spectacular, erosionally resistant ledges of silicified pumicious conglomerate (Fig. 3.22). On Vadito Hill, above the partially silicified beds of mixed provenance lie orangish and reddish beds of sandy pebble conglomerate, silty fine sand and mudstone of the upper volcaniclastic member of the Picuris Formation. Pebbles in these beds are mostly Tertiary volcanic clasts including the 25.1 Ma Amalia Tuff of the Latir volcanic field and well-rounded Proterozic quartzite. Two dated volcanic clasts from the base of this member on 'Hill 7751' to the west of Picuris Pueblo yielded ages of 19.78 Ma and 25.93 Ma (Aby et al., 2004, this volume).

Structural geology of the Peñasco embayment:
The Peñasco embayment is defined by an eastward swing in the contact between pre-Tertiary rocks and Santa Fe Group (Tesuque Formation) basin fill along the east margin of the Española Basin. The embayment is bounded by the Picuris Range on the north, the Santa Fe Range on the south, and highlands of upper Paleozoic and Proterozoic rocks east of the Picuris-Pecos fault (Fig. 3.23). Smith and Roy (2001) and Smith (2004) hypothesized that the embayment represents part of an originally more extensive area of the eastern Española Basin that remains topographically low following syn-rift uplift of the Santa Fe Range. This hypothesis calls for north- and south-plunging uplift of the Santa Fe Range by rupture of the nearly vertical Picuris-Pecos fault along the flexural hinge of the Española Basin half graben. Syn-rift uplift of the Santa Fe Range is supported by monoclinal northward tilting of Tesuque Formation along the south side of the Peñasco embayment. The top of Proterozoic rocks dips northward beneath the embayment and then rises abruptly into the Picuris Range. Basin fill sediments have mixed provenance including granitic debris from the Santa Fe Range, quartzite from the Truchas Peaks and Picuris Range, Paleozoic rocks east of the Picuris-Pecos fault, and volcaniclastic detritus comparable to the Picuris Formation. Several prominent high-level geomorphic surfaces trend northeastward across the embayment and mark Pliocene courses of the Rio Quemado, which currently drains westward from the Truchas Peaks. The progressive

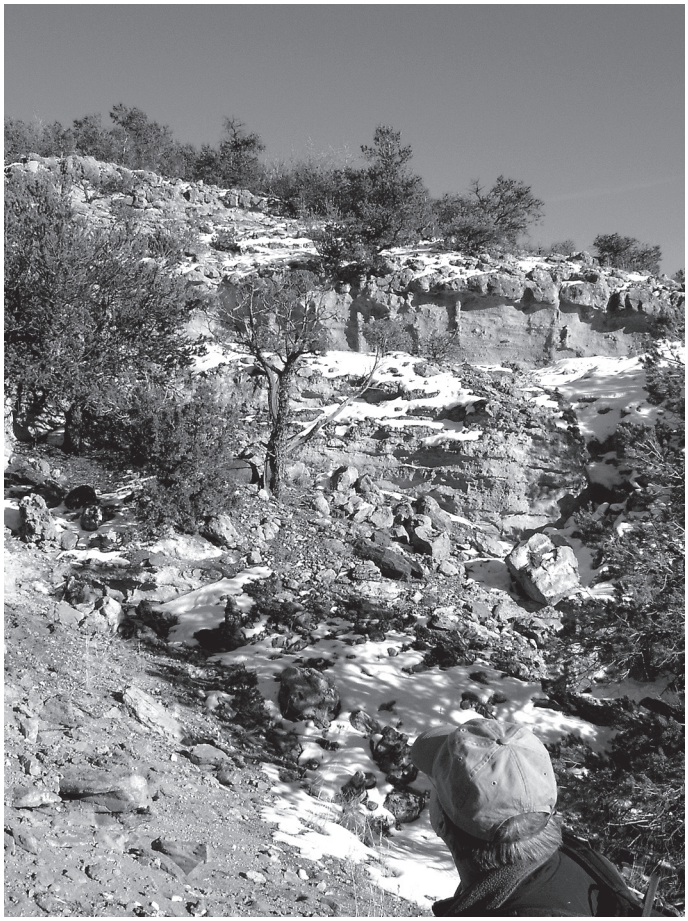


FIGURE 3.20. This view of the southern slope of Vadito hill shows interbedded ledge-forming dense conglomeratic sandstones and pebble-rich sandstones of the middle tuffaceous member of the Picuris Formation. This section is rich in moderately rounded, pebble- to cobble-size Tertiary volcanic clasts, but apparently lacks any clasts of welded Amalia Tuff. Pumice clasts near here yielded an eruptive age of approximately 27.7 Ma.

southward shift of this river is consistent with changing slopes resulting from hypothesized northward propagation of the Santa Fe Range uplift into the embayment.

Return to vehicles, retrace route to NM-75.

19.8 **Turn right on NM-75 towards Vadito and**
[49] **Peñasco**. **0.3**

20.0 Village of Vadito ('little ford' in Spanish—likely a good crossing spot along the creek). Cross the bridge over the Rio Pueblo. This valley contains late Quaternary terrace alluvium inset into and deposited on Tertiary rocks of the Santa Fe Group. The alluvium is ponded upstream of the narrow valley constriction cut into Precambrian rocks about 4 miles downstream of Vadito. **0.2**

20.2 Cerro Blanco ("white peak") at 4:00 displays the lower and middle members of the Picuris Formation (Aby et al., 2004, this volume). The white slopes are composed of the ash- and pumice-rich lower member overlain by the ledge-
forming, silica-cemented, pumice-bearing volcaniclastic member. **0.2**

21.1 Crossing the drainage divide between the Rio Pueblo valley and the Rio Santa Barbara valley. We are driving on upper Picuris Formation. High mesas along this divide preserve erosional remnants of middle Pleistocene terrace gravels (Qto) shed from the Sangre de Cristo Mountains. Sparse exposures of preserved soil profiles show stage III to stage IV calcium carbonate development. **0.9**

21.6 Entering Peñasco ("denuded valley with rocks exposed" or in the local Spanish dialect "bluff or rocky outcrop"— Julyan, 1996). The steep bluffs along the Rio Santa Barbara (to the left) are composed of sandstone and conglomerate of the Dixon member of the Tesuque Formation (middle Miocene). These conglomerates contain abundant poorly to moderately rounded clasts of Precambrian quartzite and Paleozoic sandstone, limestone, and siltstone. Sandstones characteristically contain green quartz grains. Locally, conglomerates also contain clasts of Tertiary volcanic rocks, especially in the coarser fraction, but quartzite and Paleozoic sedimentary clasts predominate throughout the Dixon member. Paleocurrent indicators (imbrication and the strike of channel walls) indicate transport from the south, southeast, and southwest (Aby et al., 2004, this volume). **0.5**

21.7 Camino Real Ranger Station on right. Just to the north of the Peñasco School buildings are excellent exposures of fluvial sandstones of uppermost upper volcaniclastic member of the Picuris Formation. **0.1**

22.1 **Junction with NM-73. Stay right on NM-75**. NM-73 follows the Rio Santa Barbara valley to the small villages of Rodarte, Llano Largo, and Llano, and to U.S. Forest Service campgrounds in the Camino Real Ranger District. For the next several miles, the highway parallels the Rio Santa Bar-

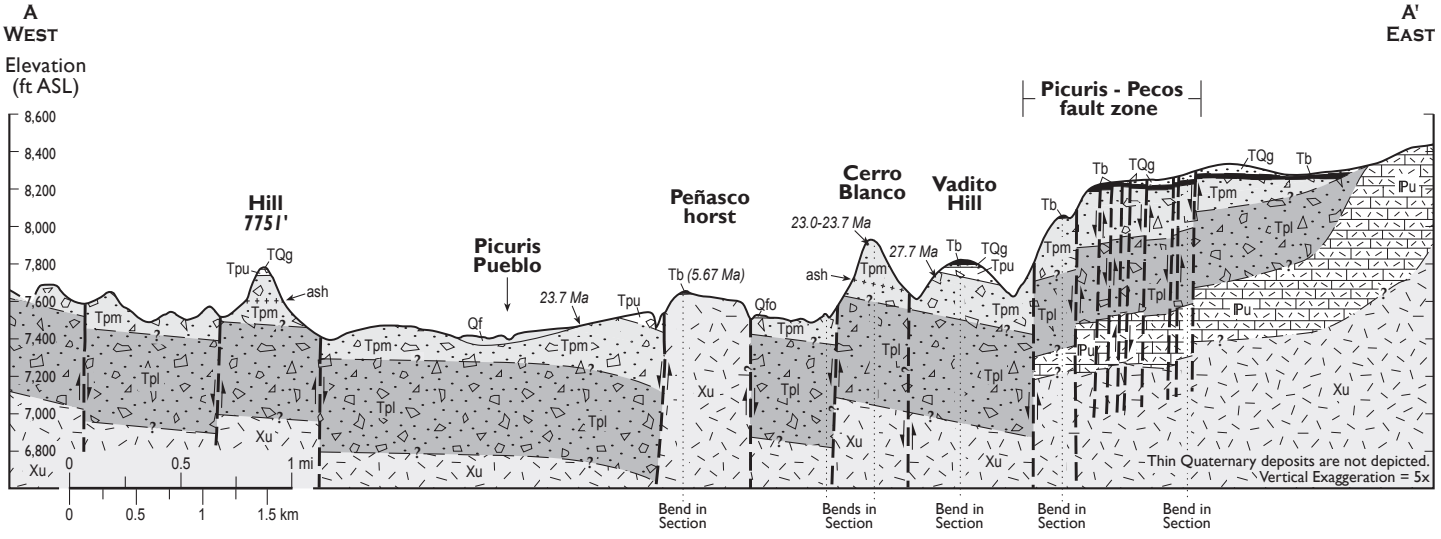


FIGURE 3.21. Generalized west-east cross section across the Peñasco quadrangle showing the principal stratigraphic units and structures. The 5.6 Ma basalt that caps Vadito hill is progressively downdropped westward by a series of north-striking normal faults that are associated with the Rio Grande rift. Many of these faults are believed to be reactivated Laramide strike-slip faults of the Picuris-Pecos fault system. Modified from a cross section by Bauer et al. (2003). Xu = Proterozoic; ℙ = Paleozoic; Tpl = lower conglomerate member of the Picuris Formation; Tpm = middle tuffaceous member of the Picuris Formation; Tb = basalt; TQg = gravel; Qf = alluvial fan.

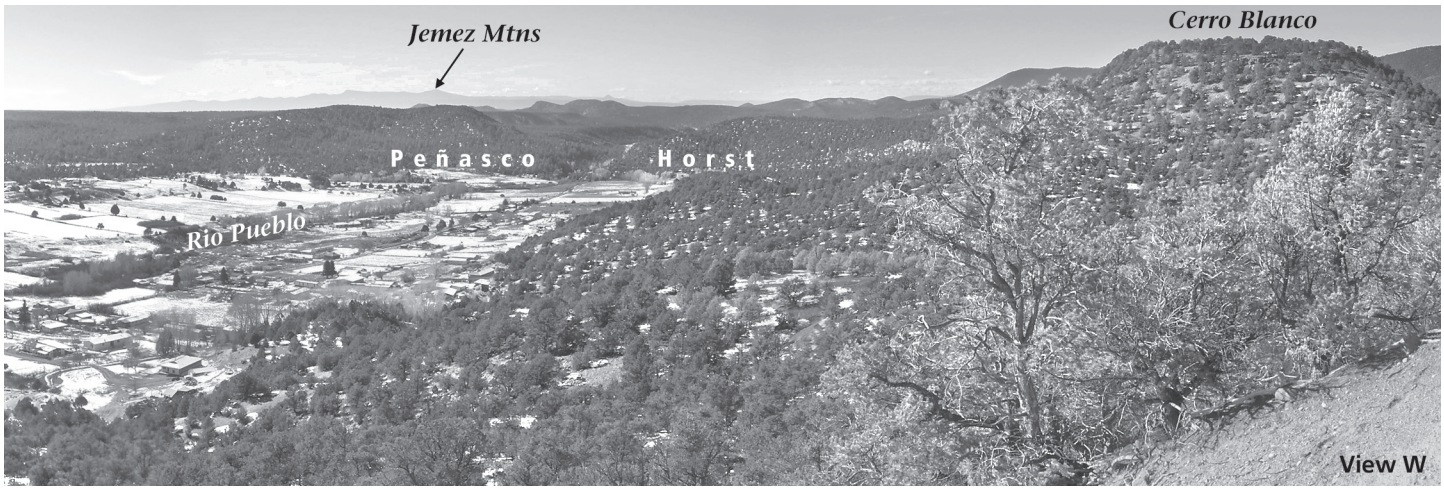


FIGURE 3.22. Panoramic view westward from Vadito Hill of the Vadito valley and Cerro Blanco. The Jemez Mountains are visible in the far distance. The rounded hills in the medium distance are composed of Proterozoic plutons of the southwestern Picuris Mountains. Note how the morphology of the Rio Pueblo changes from a wide floodplain to a narrow bedrock canyon when it encounters the Peñasco horst.

bara on late Pleistocene to Holocene stream terrace deposits (Qty). The modern drainage is inset several meters into Qty gravels. **0.4**

23.3 Proterozoic granitic outcrop on right is a southern outlier of ca. 1450 Ma Peñasco Quartz Monzonite, which is well exposed to the north and west of here (see Bauer, 1993). This biotite quartz monzonite to granodiorite is composed of quartz, plagioclase, microcline, and biotite. It commonly contains euhedral 1 mm sphene crystals. Other accessory minerals include muscovite, allanite, epidote, magnetite-hematite, apatite, and zircon. Tabular megacrysts of Carlsbad-twinned microcline up to 9 cm in length can be found locally. Myrmekite and albite rims on plagioclase are common as well. In general, this pluton is unfoliated to weakly foliated, except locally along contacts where a solid-state foliation is well developed. It is generally concordant with country rock contacts and foliation, and does not show any compositional border zone. Mafic micro-granitoid enclaves are common, especially near the pluton borders. This small exposure is evidence of a bedrock high, informally named the Peñasco horst, that extends southward from the Picuris Mountains. **1.2**

23.6 Junction with NM-76. **0.3** **[52]**

You may wish to take the highroad, NM-76, from Peñasco and drive through the scenic villages of Trampas, Truchas, and Chimayo towards Española (**see supplemental log**).

Alternatively, you may wish to proceed west on NM-75 through Peñasco, Dixon, and Embudo back to NM-68 and south to Santa Fe or north to Taos. If you are heading north, you can either backtrack to Taos, or take NM-75 and NM-518 southeast to Mora and I-25.

End of Day 3 Log

Acknowledgments

We thank Picuris Pueblo for permission to visit tribal lands. Brigitte Felix Kludt of Lemitar, NM, prepared many of the photos and figures. Sandra Azevedo and Kathy Glesener drafted geologic maps and the trip-route figure was made by David J. McCraw who also worked on several other figures.

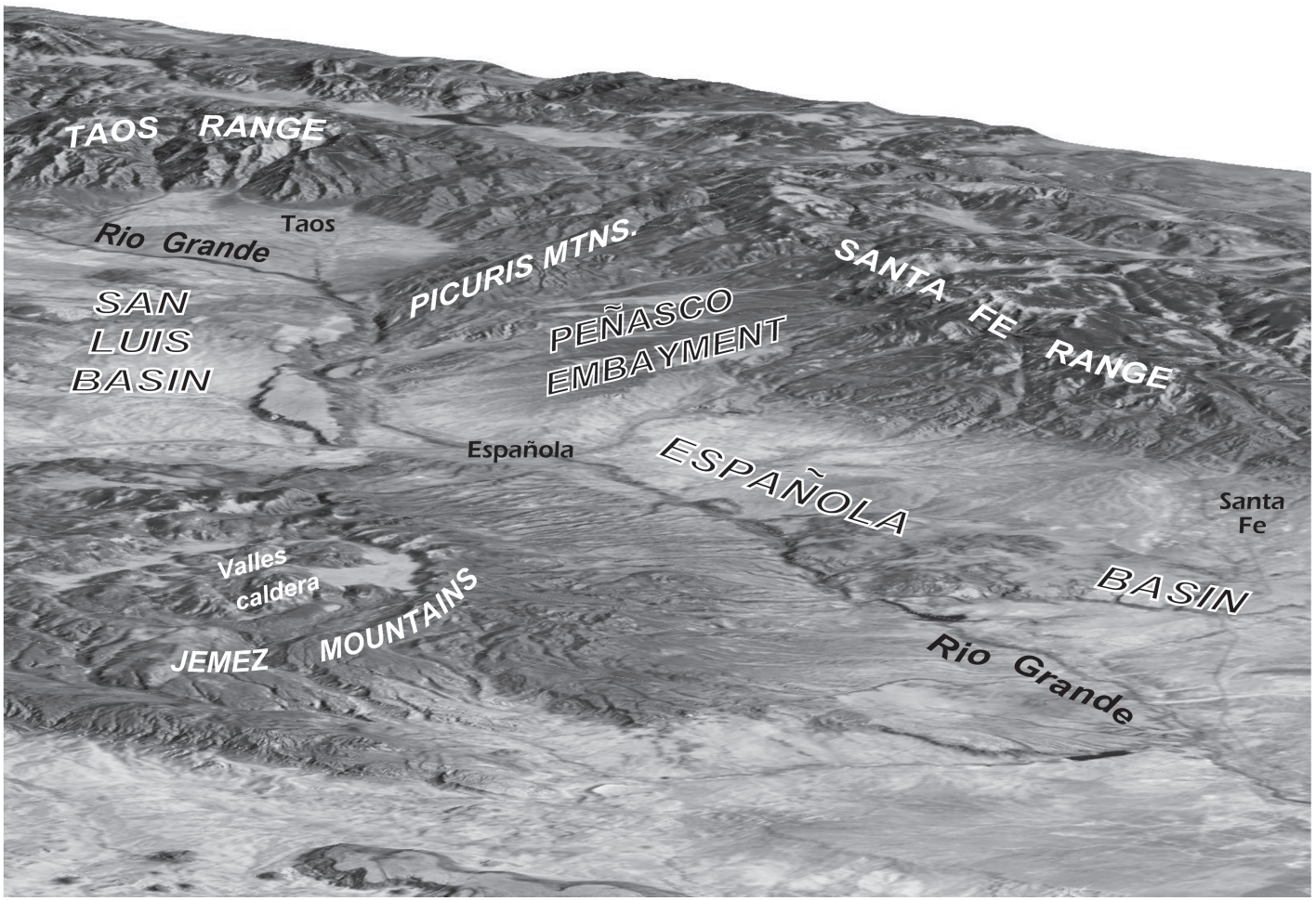


FIGURE 3.23. Oblique northeast virtual view (LANDSAT TM image — see Plate 1 — draped over DEM image) of the southern San Luis Basin and northern Española Basin showing the Peñasco embayment and nearby features.

PEÑASCO TO ESPAÑOLA
THIRD-DAY SUPPLEMENTAL ROAD LOG

DANIEL J. KONING, GARY A. SMITH, AND SCOTT B. ABY

Begin: Peñasco at intersection of NM-76 and NM-75

Distance: 30 miles

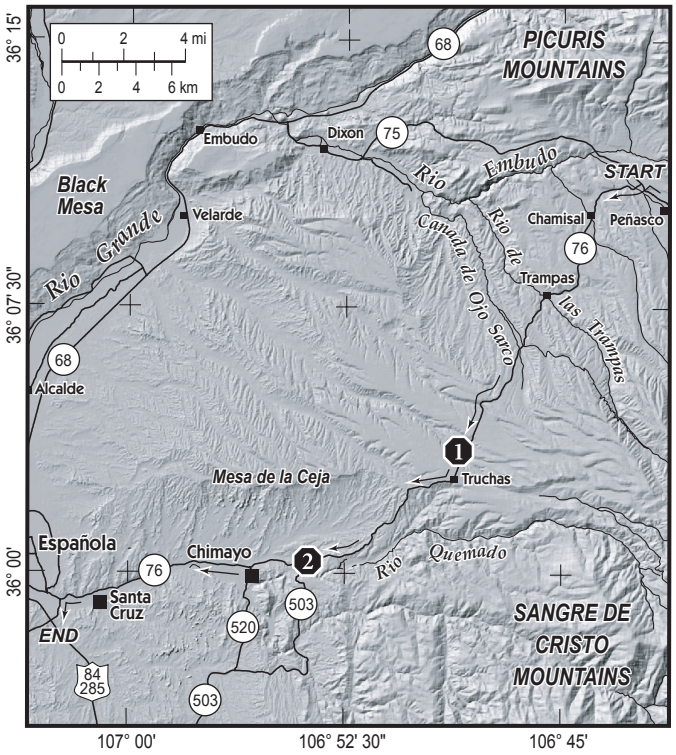
Two stops

SUMMARY

This log traverses the northeastern Española Basin and provides an interesting and scenic route for those driving towards Española. The first half of the log examines rift-fill sediments and intra-rift structures within the Peñasco Embayment north of the town of Truchas. Beyond Truchas, several exposures provide opportunity for discussion of stratigraphic, sedimentologic, and structural features within the Tesuque Formation. Additionally, there are good views of geomorphic and structural features along the western front of the Santa Fe Range.

0.0 Begin log at the intersection of NM-76 and [52] NM-75 heading south on NM-76.
For the next ~16 miles, NM-76 crosses the Peñasco Embayment, which is located between the Picuris Mountains on the north and the granitic-cored Santa Fe Range south of the town of Truchas (see Fig. 3.23). **0.0**

0.2 Holocene and late Quaternary alluvium fills the valley bottom. To the west are highlands underlain by Proterozoic granite and metasediments of the Hondo and Vadito Groups. At 4:00, at the base of Picuris Mountains, are prominent white outcrops of the Picuris Formation overlain by ~3 m of Quaternary gravel. The lower (white) part of the formation is composed of tuffaceous silt and fine sand, with interbedded gravel rich in Proterozoic Pilar Formation phyllite and Ortega Formation quartzite derived from the Picuris Mountains massif (see Bauer, 1993). These gravel beds become more common upward in the section, and may reflect concomitant uplift of the Picuris Mountains. The upper (orangish) part of the formation is composed of siltstone and sandy pebble conglomerate beds composed mostly of volcanic clasts that include Amalia Tuff (see Aby et al., 2004, this volume for complete descriptions). The presence of the 25.1 Ma Amalia Tuff indicates a provenance from the Latir volcanic field (Smith et. al., 2002; Lipman and Reed, 1989). Based on these observations, the Picuris Mountains were already a topographic high during deposition of the lower part of the Picuris Formation, but were then overtopped (at least



partially) by volcaniclastic sediment deposited by southward-flowing streams (Smith, 2004). This breaching might have been facilitated by localized down-dropping along north-south trending normal faults that have been mapped in the Picuris Mountains (these faults are shown in Bauer et al., 2003). **0.2**

0.3 Outcrop of the upper, volcanic clast-rich part of the Picuris Formation in bluffs ahead, which generally consist of coarse channel deposits together with subordinate floodplain or extra-channel sediments consisting of silt and sand. **0.1**

0.5 Junction with Acequia del Sur Road; continue [53] straight on NM-76. Approximately 0.1-0.2 miles down Acequia del Sur Road is an exposure of a fault that bounds the western side of a horst block. Immediately beyond the Acequia del Sur Road junction, on the right side of NM-76, are small exposures of silica-cemented conglomerate composed predominantly of Proterozoic granite, quartzite, amphibolite, and local Tertiary volcanic clasts. In exposures of this silica-cemented part of the Picuris Formation along the Picuris mountain front are beds containing abundant pumice clasts and/or sandy gravel composed of either Proterozoic clasts (as seen here) or Tertiary volcanic clasts. In the cliff exposures just

east of the highway here, this unit also contains a >10 m-thick sandy-silty boulder-to-pebble conglomerate composed entirely of Proterozoic clasts. This conglomerate is overlain by thinly to thickly bedded, pebbly-to-silty sand with beautifully preserved dewatering/soft-sediment deformation features. **0.2**

1.0 Outcrop on right is of the Dixon member (Steinpress, 1980), which here consists of a sand and pebble-conglomerate underlain by floodplain sediment of mud and very fine- to fine-grained sand. A fault trends subparallel to the road at the base of the cliffs to the east, and the splay exposed on Acequia del Sur Road passes under the road at this point. These two faults are west-down and merge to the south. The mesa to the west is capped by 6-12 m of sandy gravel containing boulders up to 3 m in diameter. This surficial gravel represents a high-level Quaternary alluvial deposit. **0.5**

1.8 Outcrop on right side of road consists of the Dixon member of the Tesuque Formation (here, a small channel deposit overlying fine-grained floodplain deposits). Gravelly deposits on left side of road belong to the upper part of the Picuris Formation. The volcanic clasts of the Picuris Formation serve to differentiate it from the Dixon member of the Tesuque Formation. The latter is dominated by Paleozoic limestone, sandstone, and siltstone clasts in addition to quartzite clasts. The west-bounding horst fault juxtaposes the two units at this location. **0.8**

2.2 Lucero Store in the town of Chamisal. Note that the broad alluvial valley developed in Tertiary sediments narrows abruptly approximately 2.5 km downstream, where the stream has incised into Proterozoic bedrock. This pattern is repeated in other settled tributaries of Embudo Creek, such as the Peñasco, Trampas, and Ojo Sarco drainages. Not surprisingly, settlers in the 1700s-1800s established homesteads and communities upstream from these bedrock constrictions. **0.4**

3.5 View of Truchas Peaks at 11:00. These peaks are largely composed of quartzite from the lower Ortega Formation (Miller et al., 1963). The high-level surface adjacent to the road is underlain by silt to fine sand, which are in turn underlain by Quaternary gravel. A strong calcic soil horizon is evident by the chalky appearance of the soil. **1.3**

4.2 Outcrops of the Dixon member of the Tesuque Formation are present in road-cuts on the right. The Dixon member here is composed of silt and fine sand with less than 10% coarser channel deposits. Fossil data near Dixon indicate a late Barstovian North American Land Mammal Age assemblage (14.5-11.8 Ma; Tedford and Barghoorn, 1993; Tedford et al., 1987), but the Dixon member may be older at this locality. **0.7**

5.3 Outcrops of Puntiagudo granite porphyry (Bauer and Helper, 1994) intruded by both felsic and mafic dikes. This bedrock may possibly have formed a topographic high in the middle Miocene, around which the Dixon member of the Tesuque Formation was deposited by west-southwest flowing streams. It is safest to pull off on the left side of the road if one wishes to inspect these outcrops more closely. **1.1**

5.5 On left side of the road, a photogenic wooden flume carries water for the Trampas Ditch. Enter into town of Trampas adjacent to the Rio de Trampas. Trampas was established in 1751 by 12 families from Santa Fe. **0.2**

6.3 Outcrops of fine-grained Dixon member on the right, with one cemented sandstone channel exposed. **0.8**

6.7 Roadcuts in conglomeratic Tesuque Formation here are correlated to the Dixon member. These beds consist of about equal proportions of Proterozoic quartzite and Pennsylvanian sedimentary clasts. The provenance is consistent with a river drainage basin comparable to the modern Rio Embudo. **0.4**

7.3 Roadcuts in Dixon member conglomerate, which dips about 10° to the west. Although the beds in this roadcut contain almost nothing but quartzite and Paleozoic sedimentary clasts, similar strata near the community of Ojo Sarco, 1.5 km to the northwest, contain variable abundances of volcanic clasts. The volcanic clasts are probably eroded out of the older Picuris Formation. The flat mesa visible to the west is Mesa de Cejita. Coarse gravel comprising the upper half of the visible east slope of the mesa was assigned to the Cejita Member of the Tesuque Formation by Manley (1977). Although their composition is approximately similar, the Cejita Member is overall coarser grained than the Dixon member. Along the north flank of Mesa de Cejita south of Dixon, the two gravelly members of the Tesuque Formation are separated by eolian sandstone of the Ojo Caliente Sandstone Member. Where the Ojo Caliente Sandstone is absent to the south, it is difficult to distinguish the two gravel members except in rare high-quality exposures. The top of Mesa de Cejita is an erosional remnant of the Oso geomorphic surface, described further at mile 9.7. **0.6**

7.6 Enter the Cañada de Ojo Sarco. To the east-northeast of this canyon, Proterozoic outcrops such as the one noted at mile 5.3 are common, and the contact between Proterozoic bedrock and Tertiary sediments is exposed in many places along the Cañada de Ojo Sarco. To the west-southwest of this canyon, however, exposures are entirely of Tesuque Formation strata. **0.3**

8.3 The highway exploits a relatively gentle slope that is a remnant of a once extensive hillslope geomorphic surface, which is graded to terraces along the Cañada de Ojo Sarco and rises to the forested mesa ahead. **0.7**

9.7 Here, the road crosses the Oso surface of Manley (1976a). The Oso surface is the highest and oldest of four geomorphic surfaces that record former courses of the Rio Quemado, which drains basinward from the Truchas Peaks. The

Oso surface projects close to 2.8 Ma basalt flows near Velarde (Manley, 1976a and 1976b), some 22 km to the northwest. All four of the surfaces are actually compound surfaces recording local re-grading of stream profiles during the base level drop from one surface to the next lowest one (Smith et al., 2004). The Oso surface is cut on Miocene sandy gravel of the Tesuque Formation, which is exposed in upcoming roadcuts on the highway grade. Discontinuous concentrations of quartzite boulders are the only recognizable deposits of the stream that cut the Oso surface. **1.4**

10.9 This forested mesa is the Pliocene Entrañas surface of Manley (1976a), which marks a former course of the Rio Quemado about 30 m lower than the Oso surface. Like the Oso surface, there is little in the way of unambiguous fluvial sediment associated with the cutting of the Entrañas surface on top of the coarse-grained Tesuque Formation. **1.2**

12.2 STOP 1. Overview of Peñasco Embayment.

[54] Pull out in the old roadside rest area on the right.

This stop is located at the south edge of the Entrañas surface, just above the late Pliocene Truchas surface (Manley, 1976a; Fig. S1.1). The village of Truchas is visible along the road to the south (See Fig. S1.1). The Santa Fe Range rises south of Truchas and marks the southern margin of the Peñasco embayment of the Española Basin. Looking westward is a view across the Española Basin to the Jemez Mountains. **1.3**

Smith and Roy (2001) and Smith (2004) interpret the Peñasco embayment to be part of a formerly more extensive eastern Española Basin, which has been uplifted and exhumed by Neogene uplift of the Santa Fe Range. The glaciated Truchas Peaks loom high to the southeast, and are separated from the Santa Fe Range by the north-striking Picuris-Pecos fault, along which Neogene, as well as Laramide, uplift of the Santa Fe Range is hypothesized to have occurred (Miller et al., 1963; Bauer and Ralser, 1995; Kelley, 1995; Kelley and Chapin, 1995).

The roadcuts opposite the rest area and descending the grade to the southeast are in coarse Tesuque Formation that is dipping two-to-four degrees to the northwest. The gravel contains 75-80% quartzite clasts derived from the Truchas Peaks area. The remaining clasts are granite, amphibolite, and schist that are mostly eroded from the Santa Fe Range. Pennsylvanian sedimentary rocks appear very rarely among the clasts and are derived from the east or southeast. Younger strata capping high ridges to the east are essentially 100% quartzite clasts.



FIGURE S1.1. View looking east towards the Sangre de Cristo Mountains. Town of Truchas (center) is on the Truchas surface, which is inset into the Entrañas surface (left).

This scenic view appears often in the 1988 Robert Redford movie *Milagro Beanfield War* that was adapted from the classic John Nichols novel and mostly filmed in Truchas. The towns of Truchas and Cordova, about 6 miles farther to the southwest, are the population centers for descendants of colonists of the Nuestra Señora del Rosario, San Fernando y Santiago Land Grant, which was established by Spain in 1754. The land grant encloses 14,786 acres and is owned by 290 land-grant members. About 2100 acres are irrigated to support livestock and timber harvesting produces income in the eastern and southern parts of the grant.

Return to vehicles and continue south.

13.3 The road is crossing the Truchas surface. This surface is eroded on Tesuque Formation from here to the west, and on Precambrian granitic rocks east of Truchas. A veneer of quartzite boulders, as much as 2 m across, is present across most of the surface. Looking back to the northeast there are views of a forested ridgeline that rises above the Rio de Truchas. This ridge also rises nearly 100 m above the Entrañas surface and consists of almost entirely quartzite gravel of the Tesuque Formation resting nonconformably on Proterozoic biotite-quartz monzonite and coarse-grained peraluminous granite. The ridgeline is interrupted by several beheaded valleys that were north flowing tributaries to the ancestral Rio Quemado on the Entrañas surface before piracy and incision occurred to the south in the current vicinity of the Truchas surface (Smith et al., 2004). **1.1**

13.5 T-intersection in the town of Truchas. Turn right [55] (west) to continue on NM-76. 0.2

14.1 Road-cut on right exposes coarse Tesuque Formation gravel that is compositionally similar to the deposits exposed in roadcuts below the Oso and Entrañas surfaces, although granitic and sedimentary clasts are slightly more abundant at this location. Extending beyond 3 km to the south, at 9:00 to 11:00, are a series of broad, concordant ridges developed on the lower western flank of the Santa Fe Range. Called the Borrego surface by Smith and Pazzaglia (1995), this geomorphic feature can be described as a late Miocene-Pliocene pediment approximately 8-10 km wide that appears to rise in elevation to the south (Fig. S1.2). **0.6**

14.3 Through the trees and just below the road on the left (south) is an exposure of the Guaje Pumice Bed of the Otowi Member of the Bandelier Tuff, erupted 1.61 million years

ago at the time of formation of the Valles caldera in the Jemez Mountains. The fallout pumice and ash layers rest on gravel of the Cañada Ancha surface of Smith et al. (2004). The Cañada Ancha surface is a highly degraded geomorphic surface that marks an early Pleistocene, northeasterly course of the ancestral Rio Quemado. The Cañada Ancha surface projects upslope into the sky beneath the gallery on the left, marking where the drainage was captured by an east-flowing river that paralleled the modern Rio Quemado. **0.2**

15.3 A good view to the south. At 1:00, the Borrego surface is broken by a linear north-south trending valley that marks the topographic expression of an unnamed, east-down fault (see Fig. S1.2). Preferential erosion of the softer Tesuque Formation on the hangingwall of the fault (still preserved on the north end of the fault), together with a probable weakness of the Proterozoic bedrock in the immediate area of the fault zone due to increased fracturing and shearing, has resulted in the north-south trending valley. Approximately 28 km to the south, another east-down fault appears to have experienced vertical motion around ~36 Ma, based on unpublished apatite fission-track age data (Shari Kelley, pers. comm., 2003). The fault seen here offsets the Tesuque Formation so it post-dates this sediment (inferred to be late Oligocene or later). **1.0**

15.6 Views to the northwest of badlands eroded in the Tesuque Formation. Dips in the area north of the road range from nearly horizontal to as much as 5° to the northwest and appear to decrease upsection. Although the Tesuque strata are not as well exposed here as farther west, they do clearly coarsen upward from interbedded sand, gravel, and silt to an uppermost 50 m composed almost entirely of sandy gravel, with clasts up to 80 cm across. This upward-coarsening trend is evident throughout the Española Basin (e.g., Koning and Maldonado, 2001, Koning, 2002b, Koning 2003, Smith et al., 2004). This trend is probably due to increasing rates of rift tectonism since the early Miocene, which both progressively steepened the westward tilt of the Española Basin half graben and generated more topographic relief (Koning, 2002a, 2003); however, climatic changes around 11-12 Ma may also have influenced textural trends (Koning, 2002c). At all levels in these exposures, the gravel is a mix of quartzite and granitic clasts with sparse Paleozoic sedimentary clasts; the quartzite abundance increases upsection from about 45% to 80%. The valley of Cañada de los Tanos, south of the road, follows along the southwest striking contact of Tesuque Formation with underlying Proterozoic granite, amphibolite, and schist. Good views of the Borrego surface continue to the south (Fig. S1.2). **0.3**



FIGURE S1.2. The area of low-sloping, broad, concordant ridges marks the Borrego surface developed on the western front of the Santa Fe Range (in front of and to the right of the higher mountains beneath the clouds). At extreme right is a linear north-south valley that marks the topographic expression of the unnamed, east-down fault noted in mile 15.3. View is to the south from mile 15.6.

16.3 **Junction with road to village of Cordova. Continue [56] to right on NM-76.** Both the state highway and the county road to Cordova traverse erosional surfaces graded southeastward to a prominent gravel terrace along the Rio Quemado. This terrace continues westward into the Española Valley as a high, gravel-capped pediment named the Santa Cruz surface by Manley (1976a). About two kilometers south of this junction, the Tesuque Formation rests nonconformably on Proterozoic amphibolite and biotite schist, cut by garnetiferous peraluminous leucogranite pegmatites near Cordova (Smith et al., 2004). Bedding dips in the Tesuque Formation steepen southward from 5° NNE to 16° N over a distance of less than a kilometer, suggesting that the northern terminus of the Santa Fe Range is a roughly east-west striking monoclinal flexure formed by differential uplift of the Santa Fe Range. **0.7**

18.1 At 10:00, the fault noted in mile 15.3 is marked by a steepening of the hillslope (with the higher hills in the footwall of the fault). At 11:00, this fault juxtaposes Tesuque Formation on the east with Proterozoic bedrock on the west. In a classic example of stream superposition, the Rio Quemado has maintained a relatively straight course and cut through the Proterozoic bedrock of the fault footwall, rather than going only one kilometer to the north and staying in much softer Tesuque Formation. **1.8**

18.9 Peak at 10:00, south of the narrow gorge cut by the Rio Quemado, is locally known as Cerro de Chimayó. Along its eastern side is the north-south striking Chiquito fault (east-down), estimated to have 80 to 100 m of throw. The flat surface to the east of both the fault and peak is the Santa Cruz surface; 5-25 m of sandy gravel underlies the terrace tread and is interpreted to be early Pleistocene in age (Koning et al., 2002). Straight ahead in far distance is a prominent escarpment north of the Santa Cruz River, with superb exposures of the Tesuque Formation (Fig. S1.3). Strata in the escarpment strike northeast and commonly dip 3-9° to the northwest, with dips decreasing up-section (Koning, 2003; see Minipaper by Koning). **0.8**

19.6 At 5:00, on the right side of road, is a 7-8 m-thick interval of reddish fluvial channel and overbank deposits. The channels are composed of very thin to thin beds of

GEOLOGY OF THE ESCARPMENT NORTH OF THE SANTA CRUZ RIVER, EASTERN ESPAÑOLA BASIN, AND INFERENCES REGARDING RIFT TECTONISM IN THE MIOCENE

Daniel J. Koning
New Mexico Bureau of Geology and Mineral Resources, New Mexico Tech, 801 Leroy Place, Socorro, NM 87801

One of the best exposures of the Tesuque Formation in the Española Basin is the 200 - 300 m-tall escarpment north of the Santa Cruz River and west of longitude 105°53'W (Fig. S1.3). Geologic mapping efforts here in the summer of 2002 yielded important observations of sedimentologic trends in the Tesuque Formation, which in turn allows inferences to be made regarding the nature and rates of rift tectonic activity in the Miocene (Koning, 2003). On the escarpment, eight lithostratigraphic units were differentiated in the Tesuque Formation based on provenance, texture, and general sedimentologic characteristics. Relatively good age control is obtained from fossil assemblages and tephras that are found in most units (except the oldest ones); these indicate that the strata along the escarpment probably have an age range of 30(?) to 9 Ma (Koning, 2003; Galusha and Blick, 1971; Izett and Obradovich, 2001).

The units reflect two general depositional environments. The first environment was a west- to northwest-sloping alluvial slope (see Smith, 2000, for discussion of alluvial slopes) that flanked the western margin of the Sangre de Cristo Mountains, over which flowed numerous streams with headwaters south of the Truchas Peaks. This alluvial slope environment is represented by units associated with lithosome A of Cavazza (1986). These units are characterized by medium to thick, tabular to broadly lenticular beds of silty sandstone interbedded with various proportions of coarser channel deposits of pebbly sandstone, sandstone, and pebble-conglomerate. The gravel of lithosome A is generally dominated by granite, with subordinate quartzite, and the sand fraction has abundant pinkish potassium feldspar. Lithosome A was further subdivided according to texture. Finer units (silty very fine to medium sandstone and siltstone with less than 5-7% coarser sand and gravel channel deposits) are interpreted to generally represent the distal alluvial slope. Coarser units, composed of slightly muddy very-fine to very-coarse sandstone with greater than 5-7% gravelly sand channel deposits, are interpreted to generally represent the medial and proximal alluvial slope.

The second environment was a south- to southwest-flowing fluvial system on a basin floor. This environment is represented by units associated with lithosome B of Cavazza (1986), which are characterized by siltstone, claystone, and fine sandstone floodplain deposits interbedded with subordinate, relatively broad channel deposits of sandstone and conglomerate. Sourced in the Sangre de Cristo Mountains north of Truchas Peaks and east of the Picuris-Pecos fault, the gravel of lithosome B consists of a hetereolithic clast assemblage dominated by Paleozoic sandstone, siltstone, and limestone. Subordinate clast types in this area include quartzite, granite, and felsic to intermediate volcanic clasts. The sand fraction has a grayish color (in contrast to the pinker sand of lithosome A) due to a relative abundance of lithic grains containing volcanic detritus and greenish quartz grains derived from weathering of greenish Paleozoic sandstones.

Galusha and Blick (1971) subdivided the Tesuque Formation into the Nambé, Skull Ridge, and Pojoaque Members. These members were mapped in the Cundiyo quadrangle to the south (Koning et al., 2002) and can be differentiated locally in the lower slopes of the escarpment west of Chimayó . However, it becomes increasingly difficult to map these members eastward along the escarpment because the diagnostic lithostratigraphic features associated with their respective contacts become less obvious in that direction.

Along the escarpment, strata of the Tesuque Formation generally strike northeast and unconformably overlie crystalline Proterozoic rocks. Near the mountain front, the older (upper Oligocene to lower Miocene) strata of the Tesuque Formation dip 6-10° to the northwest. As one moves up-section (i.e., to the northwest), stratal dips decrease to about 2-4°. However, major structures, such as those discussed below, can locally cause stratal dips to increase up to 47° (but generally to 8-22°).

Numerous faults offset the Tesuque Formation in the escarpment. However, three generally north-south-striking structures are particularly significant. Each is associated with normal faulting and monoclinal flexures (probably draped over normal faults at depth), The Chimayó structure has offset the western side of the Chimayó horst (the bedrock-cored topographic high present 1 to 2 km east-southeast of the old Chimayó plaza) and is crossed between miles 21.2 and 21.7 of the Day 3 Supplemental road log. This structure is down-to-the-west and manifested primarily as a monocline that is locally faulted. The Chimayó structure one to two kilometers north of Chimayó is estimated to have 90-170 m of west-down throw (includes both fault and monocline). This structure may have greater throw south of Chimayó (cross section in Koning et al., 2002). The eastern side of the Chimayó horst is bound by an east-down normal fault called the Chiquito fault (crossed at mile 21.2) that extends southward into Santa Cruz lake. Interpreted stratigraphic offset along the Chiquito fault is 80-100 m.

The third fault zone is a northward continuation of the White Operation Fault of Koning et al. (2002), which is crossed between miles 23.6 and 23.9 of the road log. This is generally a west-down structure; however, both east-down and west-down faults are present within the fault zone. The structure is manifested by a slight increase in stratal dips to 7-9° and normal faulting with about 30-40 m of interpreted throw.

Detailed sedimentologic study and mapping of the map units indicate two important trends. First, the Tesuque Formation gradually coarsens-upward since about 16 Ma, with a more pronounced, but still gradual, coarsening shortly after 12-14 Ma. This coarsening is consistent with that seen by Koning (2002a) to the southwest and Smith et al. (2004) to the east. Second, both lithosomes B and A have progressively prograded westward and northwestward since about 16 Ma (Koning, 2002c), which is

also observed to the southwest (Koning 2002a and 2002b). The favored interpretation explaining these two trends is that rift tectonism (i.e., extension) increased after about 16 Ma. This resulted in increased rates of westward tilting of the hanging wall of the Española Basin half-graben and more accommodation space being formed near the western master faults (i.e., the Pajarito fault and the prominent down-to-the-east fault south of Black Mesa), which caused the drainages associated with lithosomes A and B to shift to the west. Examples of how tilting of half-grabens may affect depositional systems is provided in Leeder and Gawthorpe (1987), Alexander and Leeder (1987), Blair and Bilodeau (1988), Mack and Seager (1990), Cather et al. (1994), and Gawthorpe and Leeder (2000).

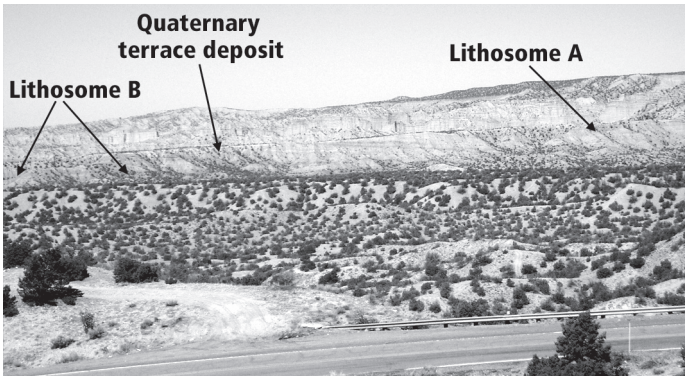


FIGURE S1.3. The ~300 m-tall escarpment north of the Santa Cruz River, as seen from STOP 2.

REFERENCES:

Alexander, J., and Leeder, M.R., 1987, Active control on alluvial architecture: Society of Economic Paleontologists and Mineralogists Special Publication 39, p. 243-252.

Blair, T.C., and Bilodeau, W.L., 1988, Development of tectonic cyclothems in rift, pull-apart, and foreland basins: Sedimentary response to episodic tectonism: Geology, v. 16, p. 517-520.

Cather, S.M., Chamberlin, R.M., Chapin, C.E., and McIntosh, W.C., 1994, Stratigraphic consequences of episodic extension in the Lemitar Mountains, central Rio Grande rift, *in* Keller, G.R., and Cather, S.M., eds., Basins of the Rio Grande Rift: Structure, Stratigraphy, and Tectonic Setting: Boulder, Colorado, Geological Society of America Special Paper 291, p. 157-170.

Cavazza, W., 1986, Miocene sediment dispersal in the central Española Basin, Rio Grande rift, New Mexico, USA: Sedimentary Geology, v. 51, p. 119-135.

Galusha, T., and Blick, J.C., 1971, Stratigraphy of the Santa Fe Group, New Mexico: Bulletin of the American Museum of Natural History, v. 144, 127 p.

Gawthorpe, R.L., and Leeder, M.R., 2000, Tectono-sedimentary evolution of active extensional basins: Basin Research, v. 12, 195-218.

Izett, G.A., and Obradovich, J.D., 2001, $^{40}Ar/^{39}Ar$ ages of Miocene tuffs in basin-fill deposits (Santa Fe Group, New Mexico, and Troublesome Formation, Colorado) of the Rio Grande rift system: The Mountain Geologist, v. 38, no. 2, p. 77-86.

Koning, D.J., 2002a, Geologic map of the Española 7.5-minute quadrangle, Santa Fe County, New Mexico: New Mexico Bureau of Geology and Mineral Resources, Open-file Geologic Map OF-GM 54, scale 1:24,000.

Koning, D.J., 2002b, Geology of the Española 7.5-minute quadrangle and implications regarding middle Miocene deposition and tectonism in the Rio Grande rift, north-central New Mexico [abstract]: New Mexico Geology, v. 42, n. 2, p. 63.

Koning, D.J., 2002c, Depositional trends of the upper Tesuque Formation, Española Basin, N.M., and inferred tectonic and climatic influences on aggradation: Geological Society of America, abstracts with programs, v. 34,n. 6, p. 281.

Koning, D.J., 2003, Geologic map of the Chimayo 7.5-minute quadrangle, Rio Arriba and Santa Fe counties, New Mexico: New Mexico Bureau of Geology and Mineral Resources, Open-file Geologic Map OF-GM 71, scale 1:24,000.

Koning, D.J., Nyman, M., Horning, R., Eppes, M., and Rogers, S., 2002, Geology of the Cundiyo 7.5-min. quadrangle, Santa Fe County, New Mexico, New Mexico Bureau of Geology and Mineral Resources, Open-file Geologic Map OF-GM 56, scale 1:24,000.

Leeder, M.R., and Gawthorpe, R.L., 1987, Sedimentary models for extensional tilt-block/half graben basins: Geological Society of London Special Publication 28, p. 139-152.

Mack, G.H., and Seager, W.R., 1990, Tectonic control on facies distribution of the Camp Rice and Palomas Formations (Pliocene-Pleistocene) in the southern Rio Grande rift: Geological Society of America Bulletin, v. 102, p. 45-53.

Smith, G.A., 2000, Recognition and significance of streamflow-dominated piedmont facies in extensional basins: Basin Research: v. 12, p. 399-411.

Smith, G.A., Gaud, M. N., and Timmons, J.M., 2004, Geologic map of the Truchas quadrangle, Rio Arriba, Santa Fe, and Taos Counties, New Mexico: NM Bureau of Geology and Mineral Resources, Open File Geologic Map OF-GM 84, scale: 1:24,000.

sand (with much reddish clay coatings on the sand grains) and gravel with clast imbrication indicating a southwest paleo-flow direction. A clast count of the gravel gives 34% granite, 25% yellowish to grayish Paleozoic limestone, 9% grayish to yellowish Paleozoic sandstone and siltstone, 14% quartzite, and minor biotite-schist, amphibolite, and quartz. This reddish sediment is somewhat similar to sediment near Santa Fe categorized as lithosome S (Read et al., 2000; Read and Koning, 2004), and may have been derived from drainages with similar provenance (east of the Picuris-Pecos fault). This reddish sediment is interbedded within the more abundant lithosome A alluvial slope sediment that is discussed in mile 19.9. Strata here strike 040-060° and dip 8-10° NW. **0.7**

19.7 STOP 2. Tesuque Formation Escarpment

[57] Carefully pull off the road on available shoulders.

Be cautious in walking alongside this curvy road because of frequent fast traffic. This stop provides a view of the prominent escarpment north of the Santa Cruz River, which offers excellent exposures of the Tesuque Formation. **0.1**

At 1:00 to 2:00, at a distance of ~ 2 km, tilted Tesuque Formation deposits are unconformably overlain by Quaternary sandy gravel deposits (Fig. S1.3). The Tesuque Formation under the gravel deposits to the left belongs to lithosome B of Cavazza (1986), and was deposited by a relatively large stream system that generally flowed south-southwest. The sediment of litho-

some B is marked by laterally extensive sandy to pebbly channel deposits and significant floodplain deposits of clay, silt, and fine sand. The clast composition of lithosome B under these terraces is approximately similar to that of the Dixon member at miles 6.3 to 7.3, and the two localities were very likely part of the same depositional system (although the lithosome B sediment here may be older than the Dixon member seen between miles 6.3 to 7.3). These lithosome B deposits interfinger to the north-northeast with lithosome A alluvial slope sediment derived from the Santa Fe Range. This interfingering relationsip suggests that the lithosome B stream had a south to slightly southeast paleo-direction at this particular locality and time of deposition. To the southwest are good views of Cerro de Chimayó and another gorge cut by the Rio Quemado (Fig. S1.4). Similar to the gorge noted at mile 18.1, this gorge is probably due to stream superimposition. Mapping by Robert Horning (in Koning et al., 2002) indicates that the Proterozoic here is composed of amphibolite and schist that have been intruded by multiple, coarse-grained granitic rocks.

Return to vehicles and continue south.

19.9 Road-cuts on right side of road provide good examples of lithosome A sediment. First used by Cavazza (1986) for arkosic and granite-rich sediment to the west-southwest, lithosome A here is marked by relatively abundant (25-60%) pebbly sandstone and sandy pebble-conglomerate channel deposits interbedded within poorly sorted, clayey-silty, very fine to very coarse sandstone deposits that are pink, light brown, very pale brown, or light yellowish brown in color. The latter, muddier sediment has been referred to as extra-channel sediment by Koning (2003) and commonly is present as thick, tabular beds that are internally massive and have been locally scoured by overlying coarser channels. The sand of lithosome A has abundant pinkish potassium feldspar, and the gravel consists of granite with minor quartz and quartzite (4-12% and 5-16%, respectively, in this area). Paleocurrent data and clast composition indicate that the granite-rich sediment was derived from the northwest part of the Santa Fe Range and deposited by west- to northwest-flowing streams on an alluvial slope (see Smith, 2000, and Kuhle and Smith, 2001 for discussion of alluvial slopes). These outcrops are interpreted to be representative of the medial or possibly proximal areas of the alluvial slope (Koning, 2003). Distal alluvial slope facies are present to the west (see comments associated with miles 23.9-25.6 of this road log). These locally have been described and subdivided in detail at the outcrop scale (Gaud, 2002; Kuhle and Smith, 2001; Kuhle, 1997) and differentiated in 1:24000-scale mapping (Koning, 2003). Strata here strike 026-072° and dip 9-13° NW. **0.2**



FIGURE S1.4. The topographic highs in the center of the photo are underlain by Proterozoic crystalline rock that includes pink granite, dark amphibolite, and a light granodiorite or tonalite that is locally foliated. Peak on the left is Cerro de Chimayó. In the foreground is the lower Tesuque Formation. The Tesuque Formation laps southward onto these topographic highs, which indicates that these highs were present during the early deposition of the Tesuque Formation in this area (probably late Oligocene to early Miocene). Locally, colluvium is present between the bedrock and the Tesuque Formation fluvial sediment. By the middle to late Miocene these topographic highs were buried by basin fill.

20.0 **Junction of NM-76 with NM-503** (which goes
[58] through the town of Rio Chiquito ~0.2 km to the south)**; continue straight on NM-76. 0.1**

21.2 Cross the Chiquito fault zone. Although no exposures of it are visible from the road, the fault can be observed 0.3 to 0.5 km to the south, where it locally juxtaposes reddish lithosome S(?) against browner lithosome A sediment. Between here and mile 21.7, stratal dips of the Tesuque Formation increase to 15 to 26° west due to a north-south mountain-front structure. This structure, called the Chimayó structure by Koning (2003), continues at least to the top of the escarpment to the north and to Cerro Piñon to the south. In its northern extent, the structure is a west-facing monoclinal-drape broken by a significant west-down normal fault along the steep mountain front at Chimayó (Koning, 2003) (Fig. S1.5). North of Chimayó 1 to 2 km, the Chimayó structure is estimated to have 90-170 m of throw (value includes both fault(s) and monocline). About 8 km to the south of Chimayo, a cross-section by Koning et al. (2002) suggests a possible structural relief on the scale of 1000 m. In that area, there is no west-down fault exposed at the surface and the top of the monoclinal drape is not preserved due to erosion. Even though faults and monoclines do coincide with much of the lower western front of the Santa Fe Range (west of the Borrego surface), the gross structure of the Española Basin southeast of the Abiquiu embayment is still probably that of a west-tilted half-graben (Cordell, 1979; Manley, 1979a; and Biehler et al., 1991). **1.2**

21.7 **Intersection of NM-76 with NM-520; continue**
[59] **straight on NM-76**. Chimayó is a small town whose historic center lies immediately southwest of this intersection. Thousands of pilgrims walk to the Santurario de Chimayó (0.9 miles to the south) from throughout northern New Mexico during Easter weekend. The church is built on sediment ascribed to have miraculous healing powers that pilgrims can scoop from the floor. Aside from the church, Chimayó is best known for its weaving products and for the Chimayó green chili—a unique, small, and relatively mild chili grown locally.



FIGURE S1.5. Looking north-northeast to the topographic high underlain by Proterozoic bedrock north of Cerro de Chimayó (see Fig. S1.4). The Santa Cruz River near the Santuario de Chimayó lies in the foreground. The gorge in the mountain front marks the Rio Quemado, probably formed due to stream superimposition. Note the pronounced change in slope on the western (left) side of the topographic high north of the Rio Quemado. Here, the upper slope forms a relatively broad surface dipping 8-15° W-NW. This slope value is similar to the general stratal dips of the Tesuque Formation and may represent an exhumed erosional surface developed in the middle(?) Miocene. The lower slope steepens significantly to 20-30° and coincides with a prominent west-down fault of the Chimayó structure

The book *Sabino's Map* by Don Usner (1995) provides colorful recollections of the area's early days. **0.5**

22.3 Highway NM-76 follows the Santa Cruz River westward between Chimayó and Española, and generally passes over late Holocene alluvium. In bluffs about 0.5 km to the north and 1 km to the south, Lithosomes A and B are present in an interfingering relationship. This sediment belongs to the Nambé Member of the Tesuque Formation, as established by Galusha and Blick (1971). Between here and mile 23.6, several faults project across the highway from outcrops north and south of the valley (Koning, 2003; Koning et al., 2002). **0.6**

23.6 The White Operation fault zone underlies Quaternary alluvium in this vicinity (Koning et al., 2002; Koning, 2003). This structure is manifested by a slight increase in stratal dips and exposures of several strands of normal faults (generally west-down). In the badlands to the north, there is an estimated 30 m of down-to-west throw across this structural zone; 1.4 km to the southwest, there is approximately 70-to-80 m of throw based on the juxtaposition of certain ash beds. Across the Santa Cruz River 1.9 km to the south (9:00), one can see an ash bed near the top of the ridge. This is White Ash #2 of the Skull Ridge Member (see Galusha and Blick, 1971). Like White Ash #4 (mile 23.9 and mile 24.9), this ash serves as a wonderful stratigraphic marker, largely because of a sedimentologic change that occurs across it (see Kuhle and Smith, 2001). An $^{40}Ar/^{39}Ar$ date of 15.5 Ma has been obtained from White Ash # 2 (Izett and Obradovich, 2001). The ashy bed 35-40 m below White Ash #2 is White Ash #1, the base of which serves as the contact between the Skull Ridge and Nambé Members of the Tesuque Formation (Galusha and Blick, 1971). A couple of meters above this ash is the late Hemingfordian - early Barstovian North American Land Mammal age boundary (Galusha and Blick, 1971; Tedford and Barghoorn, 1993; Tedford et al., 1987). North of the highway, White Ash #1 does not occur so the contact between the Skull Ridge and Nambé Members cannot be adequately mapped there. **1.3**

23.9 The prominent white ash on top of the bluffs 1 km to the south (about 10:00) is White Ash #4 of the Skull Ridge Member of the Tesuque Formation. In this area, White Ash #4 is underlain by medium to thick, tabular beds of siltstone and very fine to fine sandstone with minor sandy channels of lithosome B, and overlain by more arkosic fine sand of the basin floor - distal alluvial slope transition (see Koning, 2003). This ash is probably the most laterally extensive of the ashes in the Tesuque Formation, is relatively thick (70 to 250 cm), and serves as a useful stratigraphic marker bed. It has been dated at 15.45 Ma and 15.3 Ma using $^{40}Ar/^{39}Ar$ methods (McIntosh and Quade, 1995, and Izett and Obradovich, 2001, respectively). The White Operation fault lies between White Ash #4 here and White Ash #2 noted at mile 23.6. **0.3**

24.9 A short distance ahead (0.1 miles) on right side of road, is a 50-65 cm-thick fine white ash that is interbedded within pinkish, well-consolidated siltstone and very fine-grained sandstone. **It is dangerous to closely inspect this outcrop because the shoulder of the road is virtually non-existent here.** This ash is tentatively correlated to the White Ash #4 of the Skull Ridge Member. The ash is truncated on its western end by a west-down fault. The fine-grained nature of the Tesuque Formation in this area represents basin floor facies and transitional basin floor-distal alluvial slope facies, and contrasts with the coarser, more proximal alluvial slope facies seen in mile 19.9. Here and to the west, bluffs of Tesuque Formation adjacent to the road on the north are unconformably overlain by a Quaternary sand and gravel deposit up to 18 m thick. The basal 2-4 m is composed of grayish, clast-supported cobbles with abundant quartzite (about subequal to granite in abundance). The overlying sediment is generally fine-grained, but has about 25-35% coarse channel deposits with a clast assemblage dominated by granite. The age of this terrace deposit is interpreted to be ~120-150 ka, based on correlation with terraces west of the Rio Grande whose ages have been constrained by carbon-14 and amino-acid epimerization ratio chronologic data (Dethier and McCoy, 1993; Dethier and Reneau, 1995; Koning and Manley, 2003). **1.0**

25.3 Over the next 200 m, the road parallels the strike of bedding and outcrops on the right offer exposure of transitional basin-floor to distal alluvial-slope facies. Near the base of the slope, a sandy channel complex is interbedded in siltstone and very fine sandstone similar to that at mile 24.9. The sand is relatively arkosic and pink here (with an estimated

1:4 ratio of lithic grains to pinkish potassium feldspar) but has a higher proportion of Paleozoic(?) lithics (about subequal compared to pink potassium feldspar grains) and a grayer color 200-300 m to the southwest. This gradation of color and sand composition is characteristic of the eastern part of the basin floor facies where it grades eastward into distal alluvial slope facies of the Tesuque Formation (i.e., the transition between lithosomes B and A). This lateral gradation reflects input of arkosic sand from relatively small, west- to northwest-flowing, tributary alluvial slope drainages into the southwest-flowing lithosome B fluvial system. The contact between the Skull Ridge and Pojoaque Members of Galusha and Blick (1971) has been placed at the base of this channel complex by Koning et al. (2002), although exact correlation with the "type locality" of this contact 3.8 km to the southwest (in a roadcut at La Puebla, see Galusha and Blick, 1971) is not certain. **0.4**

25.6 To the right is a 30 cm-thick fine white ash. The ash is altered and interbedded within medium, tabular beds of siltstone associated with the transition between basin-floor to alluvial-slope facies. There are over 70 tephra beds in the Santa Fe Group basin fill. The presence of so many tephra beds, together with generally good exposure, makes the Española Basin an ideal locality for stratigraphic studies of basin fill in a rift half-graben setting. Fossils collected between here and Española are associated with the Late Barstovian North American Land Mammal Age (14.5-12 Ma; Tedford and Barghoorn, 1993; Tedford et al., 1987). **0.3**

25.7 Exposures of very fine-to-fine, arkosic sandstone and silty sandstone. Strata here generally strike 030-050° and dip 4° NW. With one exception (mile 27.8), between here and Española there are no significant faults observed in the Tesuque Formation near the highway. **0.1**

25.8 Approximately 6-10 m up the hill to the north is a relatively unaltered, light gray ash. **0.1**

26.2 Intersection with road to La Puebla; continue straight
[60] on NM-76. **0.4**

26.4 Crossing Arroyo Quarteles. About 1 km up this arroyo are good exposures demonstrating the westward lateral transition from distalmost lithosome A alluvial slope facies to lithosome B fluvial channels and floodplain deposits. West of here, the Tesuque Formation observed near the road is interpreted as lithosome B basin floor facies and has an interpreted age of 14-12 Ma. **0.2**

27.0 Sandy gravel associated with the terrace described at mile 24.9 caps the bluffs to the right of the road. In this area, the underlying basin floor facies are relatively sandy. **0.6**

27.7 Basin floor sediment here is generally composed of massive, arkosic, very fine to fine sand, with some channels of medium- to very coarse-grained sand and minor pebbles of lithosome B provenance. The finer sand may perhaps be eolian. **0.7**

27.8 Outcrop on right exhibits fault displacement of silty very fine- to fine-grained sandstone and mudstone. This fault is part of the west-down Road fault of Galusha and Blick (1971) which appears to change to an east-down sense of motion) about 5 km north of here (Koning and Manley, 2003). **0.1**

28.3 **Junction with NM-106. Turn left (south) on NM-**
[61] **106** and pass over late Holocene valley fill. **0.5**

28.5 Sikh Gurdwara on west side of road. Founded in 1972 based on Sikh spiritual principles, this community of greater then 300 Sikhs run businesses, raise families, and meditate in a spirit of togetherness. **0.2**

28.8 Intersection with East Sombrillo Road (County Road 40). Just 0.1 mile east on this road are good exposures of lithosome B fluvial basin floor sediment, which here is generally composed of channel-fill sand and pebbly sand with 5-7% floodplain deposits of clay to silt. The pebbles are mostly Paleozoic limestone, sandstone, and siltstone, but subordinate quartzite and intermediate to felsic volcanic clasts are also present. Other outcrops of lithosome B in the vicinity are also generally dominated by sand. Two minor west-down faults can be observed. This sediment is still part of the Pojoaque Member of the Tesuque Formation. About 0.2 miles down East Sombrillo Road is an interesting Sikh temple. **0.3**

30.0 **Junction of NM-76 with US-285**. **1.2**
[62] Turn left (southeast) on US-285 to travel to Santa Fe and further south or turn right to head back to Taos or to points further north.

END OF SUPPLEMENTAL ROAD LOG.